Supplemental Information

Hydrogen Activation by Biomimetic [NiFe]-Hydrogenase Model Containing Protected Cyanide Cofactors

Brian C. Manor and Thomas B. Rauchfuss*

School of Chemical Sciences, University of Illinois

Table of Contents

Additional Synthetic Procedures

Isomerization of 1(BAr$^F_3$)$_2$. A solution of the cis-CO/trans-CN isomer of **1**(BAr$^F_3$)$_2$ (10 mg, 0.006 mmol) in CD_2Cl_2 (1 mL) was loaded into an NMR tube fitted with a J Young valve and irradiated by a 365 nm LED array for 3h. ^{19}F and ^{31}P NMR measurements showed conversion of the initial isomer to a 3:1 ratio of the trans-CO/cis-CN and cis-CO/cis-CN isomers. Upon sitting in the absence of light for 5 days, the mixture shifted to a 1:25 ratio of the trans-CO/cis-CN and cis-CO/trans-CN isomers.
trans-CO/cis-CN: IR(CH_2Cl_2): ν_{CN} = 2215, 2201 cm^{-1}, ν_{CO} = 2087(w), 2030 cm^{-1}. ^{31}P NMR (CD_2Cl_2): δ 58.7 (s). ^{19}F NMR (CD_2Cl_2): −135.2 (d, o-F), −160.6 (t, p-F), −166.5 (t, m-F).
cis-CO/cis-CN: IR(CH_2Cl_2): ν_{CN} = 2214, 2202 cm^{-1}, ν_{CO} = 2070, 2020 cm^{-1}. ^{31}P NMR (CD_2Cl_2): δ 58.9, 58.5 (AB quartet, J_{PP} = 37 Hz). ^{19}F NMR (CD_2Cl_2): −135.0 (d, o-F), −135.1 (d, o-F), −160.0 (t, p-F), −160.7 (t, p-F), −166.0 (t, m-F), −166.5 (t, m-F).

Isomerization of 2(BAr$^F_3$)$_2$. A solution of the cis-CO/trans-CN isomer of **2**(BAr$^F_3$)$_2$ (10 mg, 0.006 mmol) in CD_2Cl_2 (1 mL) was loaded into an NMR tube fitted with a J Young valve and irradiated by a 365 nm LED array for 2 h. ^{19}F and ^{31}P NMR showed conversion of the initial isomer to the trans-CO/cis-CN isomer. No further isomerization was observed upon standing in the absence of light. IR(CH_2Cl_2): ν_{CN} = 2214, 2200 cm^{-1}, ν_{CO} = 2084(w), 2027 cm^{-1}. ^{31}P NMR (CD_2Cl_2): δ 75.1 (s). ^{19}F NMR (CD_2Cl_2): −135.0 (d, o-F), −160.4 (t, p-F), −166.2 (t, m-F).

Borohydride Route to Et$_4$N[(CO)(CNBAr$^F_3$)$_2$Fe(pdt)(H)Ni(dppe)], Et$_4$N[H3(BAr$^F_3$)$_2$] (alternative to the H$_2$ route). A solution of **1**(BAr$^F_3$)$_2$ (100 mg, 0.057 mmol) in 10 mL of CH_2Cl_2 was treated with 1.2 mL (1.2 equiv.) of a stock solution of Me_3NO in CH_2Cl_2 (0.057 M) causing the solution to darken in color. The solution was quickly treated with a suspension of Et_4NBH_4 (8.3 mg, 0.057 mmol) in 10 mL CH_2Cl_2 and stirred for 30 minutes. The solvent was removed under reduced pressure and the resulting solid was extracted into 20 mL of Et_2O and the mixture was passed through Celite. Once the solution was concentrated to approximately 3 mL, pentane (20 mL) was added, forming a brown solid which was isolated by filtration. The remaining workup is similar to that described with Me_3NO and H_2. Yield: 22 mg (21%). Crystals suitable for x-ray diffraction were grown by diffusion of pentane into a solution of Et$_4$N[H**3**(BAr$^F_3$)$_2$] in dichloromethane at 0°C.

Et$_4$N[(CO)(CNBAr$^F_3$)$_2$Fe(pdt)(H)Ni(dcpe)], Et$_4$N[H4(BAr$^F_3$)$_2$]. In a thick-walled glass pressure tube, a solution of **2**(BAr$^F_3$)$_2$ (140 mg, 0.0789 mmol) in CH_2Cl_2 (10 mL) was treated with Me_3NO (7.1 mg, 0.0946 mmol) in 2 mL of CH_2Cl_2 and immediately frozen by inserting the tube into liquid nitrogen. The headspace was evacuated and refilled with 40 psig of H_2, and the solution was thawed. After stirring this mixture for 2 h, solvent was removed and the residue was extracted into Et_2O. The extract was filtered through Celite and the solvent removed under vacuum. ^{19}F NMR analysis showed ~50% of signals product. The crude sample was dissolved in 10 mL of CH_2Cl_2 and treated with excess Et_4NCl (131 mg, 0.789 mmol). The solvent was removed under vacuum, and the product was extracted into 10 mL Et_2O. The mixture was filtered through Celite, and the filtrate was dried under vacuum. The solid was dissolved in a minimal amount of THF and loaded onto a column of neutral alumina (Brockmann Level IV) eluting THF. The first

red band was discarded, and the remaining brown band was eluted with CH_2Cl_2. The solution was concentrated to 5 mL, layered with 20 mL of pentane, and cooled to −30 °C precipitating an oil. Upon storing under vacuum, the oil converted to a solid. The solid recrystallized from 5 mL of CH_2Cl_2, layered with 20 mL of pentane and cooled in a −30 ºC, yielding red crystals (49 mg, 33%).

Synthesis of $HNMe_3BAr^{F24}$. Me_3N•HCl (54 mg, 0.56 mmol) and $NaBAr^{F24}$ (500 mg, 0.56 mmol) were dissolved in CH_2Cl_2 (40 mL) and stirred for 10 min. The solvent was removed under vacuum forming an off-white solid. The product was extracted into Et_2O (40 mL), passed through Celite, and the solvent was removed under vacuum. The product was crystallized from CH_2Cl_2 and hexanes at 0°C. Yield 0.44 g (84%). ^{1}H NMR (CD_2Cl_2): 7.72 (s, 8H); 7.57 (s, 4H); 6.38 (t, 2H, *H*N$(CH_3)_3$, J_{NH} = 55 Hz); 3.05 (d, 9H, HN(C*H*$_3)_3$).

Synthesis of Pyrrolidinium BAr^{F24} (Pyr•$HBAr^{F24}$). Pyrrolidine (64 mg, 9.0 mmol) was dissolved in CH_2Cl_2 (10 mL) and treated with HBF_4•Et_2O (1.3 mL, 9.0 mmol) and stirred for 30 minutes. The solvent was removed under vacuum producing a white powder. The solid was washed with pentane (20 mL) and Et_2O (20 mL) and dried under vacuum. Yield 1.32 g (92%). [Pyrrolidinium]BF_4 (36 mg, 0.226 mmol) and $NaBAr^{F24}$ (200 mg, 0.226 mmol) were combined and dissolved in CH_2Cl_2 (40 mL) and let stir for 1 h. The solvent was removed under vacuum, producing an oil. An ether extract of this oil (10 mL) was passed through Celite, and the solvent was removed under vacuum. The resulting oil was triturated with pentane producing an off-white solid. The solid was dissolved in CH_2Cl_2 (5 mL), layered with pentane (20 mL) and cooled to 0 °C yielding white crystals (0.19 g, 90%). ^{1}H NMR (CD_2Cl_2): 7.72 (s, 8H); 7.57 (s, 4H); 6.14 (t, 2H, H_2N, J_{NH} = 53 Hz); 3.58 (s, 4H, N(C$H_2)_2(CH_2)_2$); 2.20 (s, 4H, N$(CH_2)_2$(C$H_2)_2$.

Synthesis of $[PhNH_3]BAr^{F24}$·$2Et_2O$. $[PhNH_3]BF_4$ (41 mg, 0.226 mmol) was dissolved in MeCN (5 mL) and this solution was treated with a solution of $NaBAr^{F24}$ (200 mg, 0.226 mmol) in MeCN (5 mL). The mixture was stirred for 10 min, followed by removal of the solvent. The product was extracted into Et_2O (10 mL) and passed through Celite, and the filtrated was dried under vacuum. The resulting off-white solid was dissolved in CH_2Cl_2, layered with pentane, and cooled to −30 °C, yielding white crystals (210 mg, 83%). Two molecules of Et_2O were found by ^{1}H NMR and were not able to be removed even after drying the sample under vacuum for 24 h. ^{1}H NMR (CD_2Cl_2): 8.69 (br, 3H, *H*$_3$NPh); 7.72 (s, 8H); 7.63-7.61 (m, 3H, H_3N*Ph*); 7.56 (s, 4H); 7.35-7.33 (m, 2H, H_3N*Ph*); 3.57 (m, 8H, $(CH_3CH_2)_2O$); 1.17 (m, 12H, $(CH_3CH_2)_2O$).

Titration of $Et_4N[H3(BAr^F{}_3)_2]$ with $HNMe_3BAr^{F24}$. A sample of $Et_4N[H$**3**$(BAr^F{}_3)_2]$ (2.6 mg, 0.0014mmol) was dissolved in 1 mL of CD_2Cl_2. A standard solution of $HNMe_3BAr^{F24}$ was prepared by dissolving 130 mg of $HNMe_3BAr^{F24}$ (0.14 mmol) in 1mL of CD_2Cl_2 (0.14 M). A 1H NMR spectrum was collected before addition of $HNMe_3BAr^{F24}$ and after each addition. The sample was kept cold between acquisitions to prevent decomposition and warmed to room temperature immediately prior to recording the ^{1}H NMR spectrum.

Titration of $Et_4N[H4(BAr^F{}_3)_2]$ with Pyr•$HBAr^{F24}$. A sample of $Et_4N[H$**4**$(BAr^F{}_3)_2]$ (2.5 mg, 0.0013 mmol) was placed in a J Young NMR tube and dissolved in 0.9 mL of CD_2Cl_2. A standard

solution of Pyr•HBAr^{F24} was prepared by dissolving 62 mg of Pyr•HBAr^{F24} (0.067 mmol) in 1 mL of CD_2Cl_2 (0.067 M). A ^{1}H NMR spectrum was collected before addition of Pyr•HBAr^{F24} and after each addition. The sample was kept cold between acquisitions to prevent decomposition and warmed to room temperature immediately prior to recording the ^{1}H NMR spectrum.

Production of H_2 by protonation of $Et_4N[H3(BAr^F{}_3)_2]$ with $PhNH_3BAr^{F24}\cdot 2Et_2O$. Three vials were loaded with a known amount of $Et_4N[H\mathbf{3}(BAr^F{}_3)_2]$ (~3 mg) and 0.5 of CH_2Cl_2 and sealed with a rubber septum. A stock solution of acid was prepared from $PhNH_3BAr^{F24}\cdot 2Et_2O$ (60 mg, 0.0054 mmol) in 1.75 mL of CH_2Cl_2. An aliquot of 0.5 mL of stock solution of acid was injected through the septum, resulting in a color change of the solution from brown to orange. An internal standard of 100 µL of CH_4 was injected through the septum into the headspace of the vial. Each vial was allowed to stir for at least 30 minutes before the headspace was analyzed by gas chromatography.

Table S1. IR and ^{31}P NMR Aignals for Dicarbonyl Complexes **1** and **2** and Their bis-BAr^F_3 Adducts and Isomers Thereof (CH_2Cl_2 solution).

Compound	**ν_{CN} (cm^{-1})**	**ν_{CO} (cm^{-1})**	**^{31}P NMR (ppm)**
$(CO)_2(CN)_2Fe(pdt)Ni(dppe)$ (**1**) cis-CO, trans-CN	2110, 2081	2053, 2005	56.9
$(CO)_2(CN)_2Fe(pdt)Ni(dcpe)$ (**2**) cis-CO, trans-CN	2113, 2090	2045, 1995	66.3
isomer of **2** cis-CO, cis-CN	2120	2033, 1982	67.8, 66.5 (J_{PP} = 33 Hz)
$(CO)_2(CNBAr^F_3)_2Fe(pdt)Ni(dppe)$ [**1**$(BAr^F_3)_2$] cis-CO trans-CN	2194, 2166	2088, 2050	56.4
1$(BAr^F_3)_2$ trans-CO, cis-CN	2215, 2201	2087 (w), 2030	58.7
1$(BAr^F_3)_2$ cis-CO, cis-CN	2214, 2202	2070, 2020	58.9, 58.5 (J_{PP} = 37 Hz)
$(CO)_2(CNBAr^F_3)_2Fe(pdt)Ni(dcpe)$ [**2**$(BAr^F_3)_2$] cis-CO trans-CN	2190, 2149	2085, 2046	69.8
2$(BAr^F_3)_2$ trans-CO, cis-CN	2214, 2200	2084 (w), 2027	75.1
2$(BAr^F_3)_2$ cis-CO, cis-CN	2210	2068, 2030	70.2, 69.5 (J_{PP} = 30 Hz)

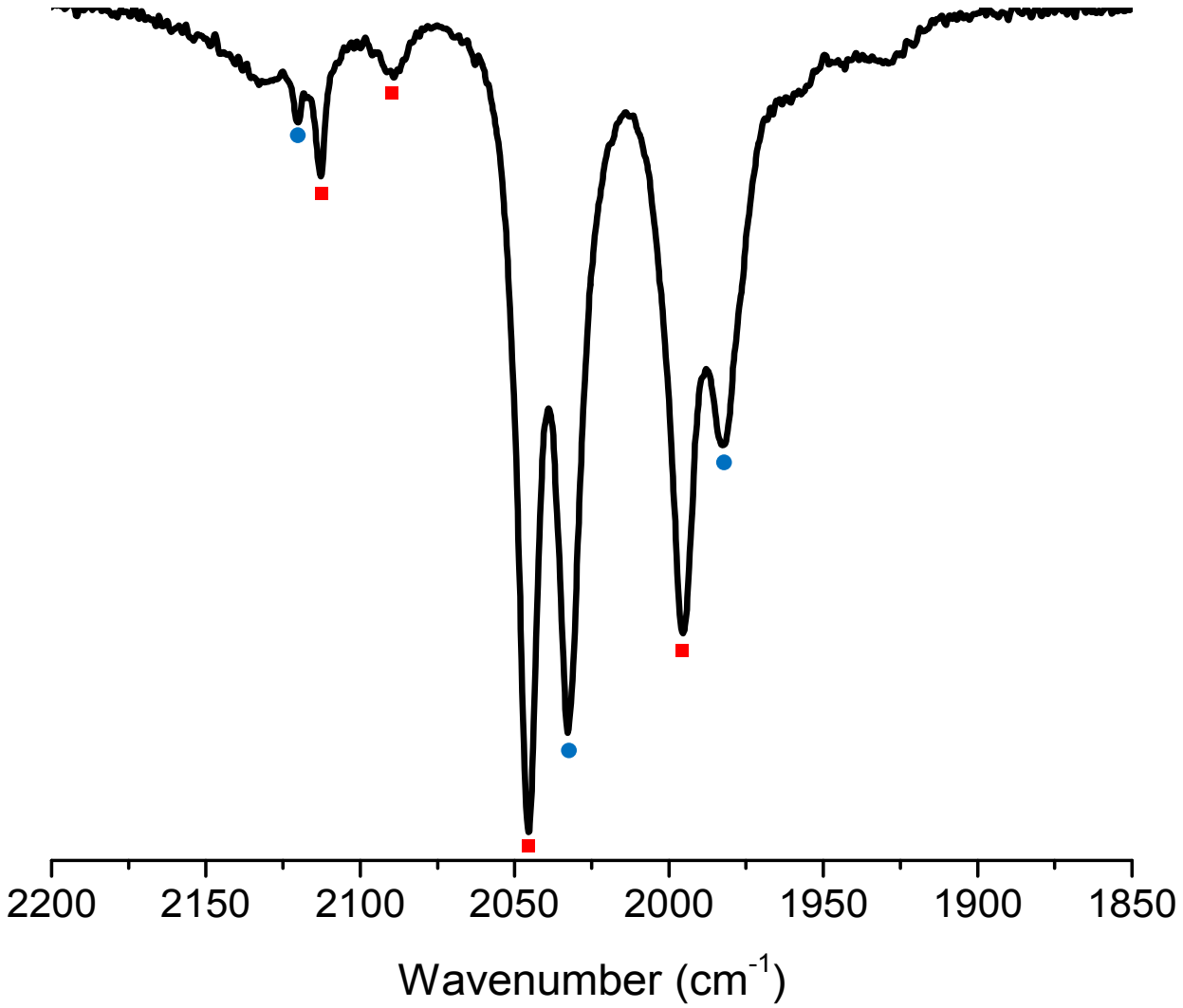

Figure S1. IR spectrum of cis-CO/trans-CN(■) and cis-CO/trans-CN(●) isomers of **2** in CH_2Cl_2 solution. The second expected ν_{CN} for the cis-CO/cis-CN isomer is obscured.

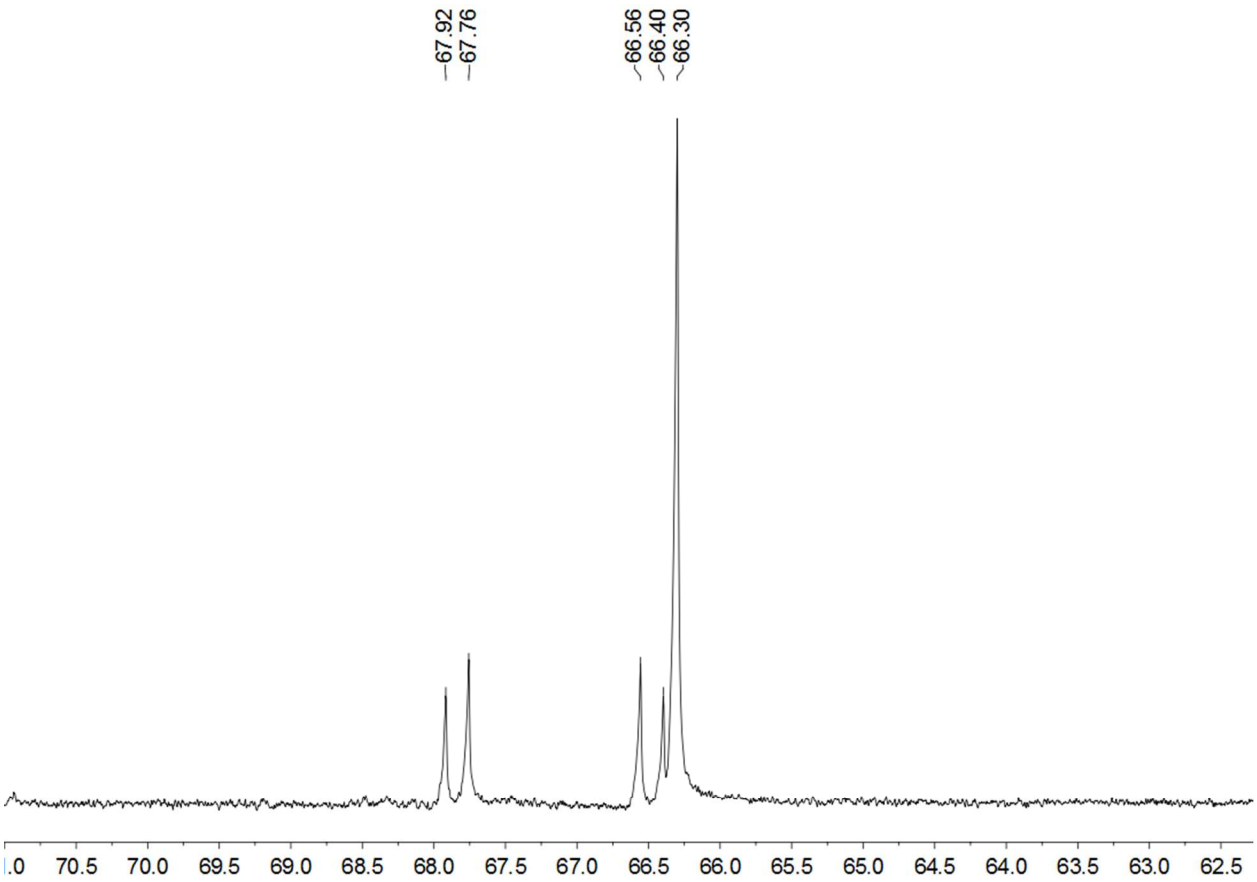

Figure S2. ^{31}P NMR spectrum of the cis-CO/trans-CN and cis-CO/trans-CN isomers of **2** in a CD_2Cl_2 solution.

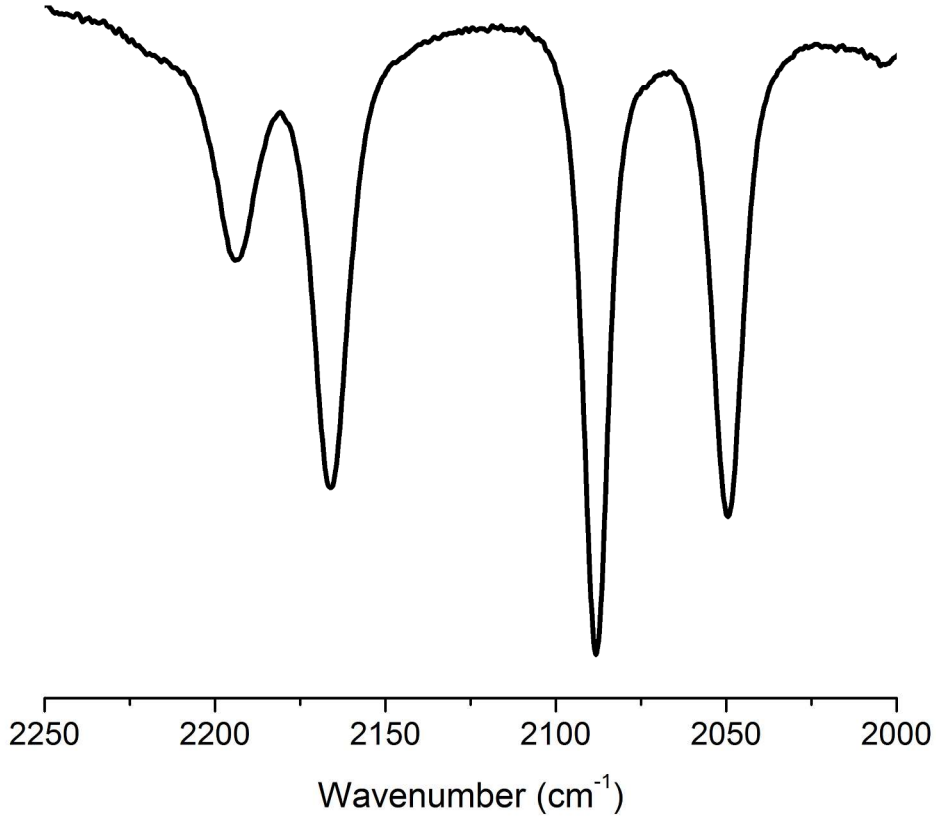

Figure S3. IR spectrum of the cis-CO/trans-CN isomer of **1**$(BAr^F{}_3)_2$ in a CH_2Cl_2 solution.

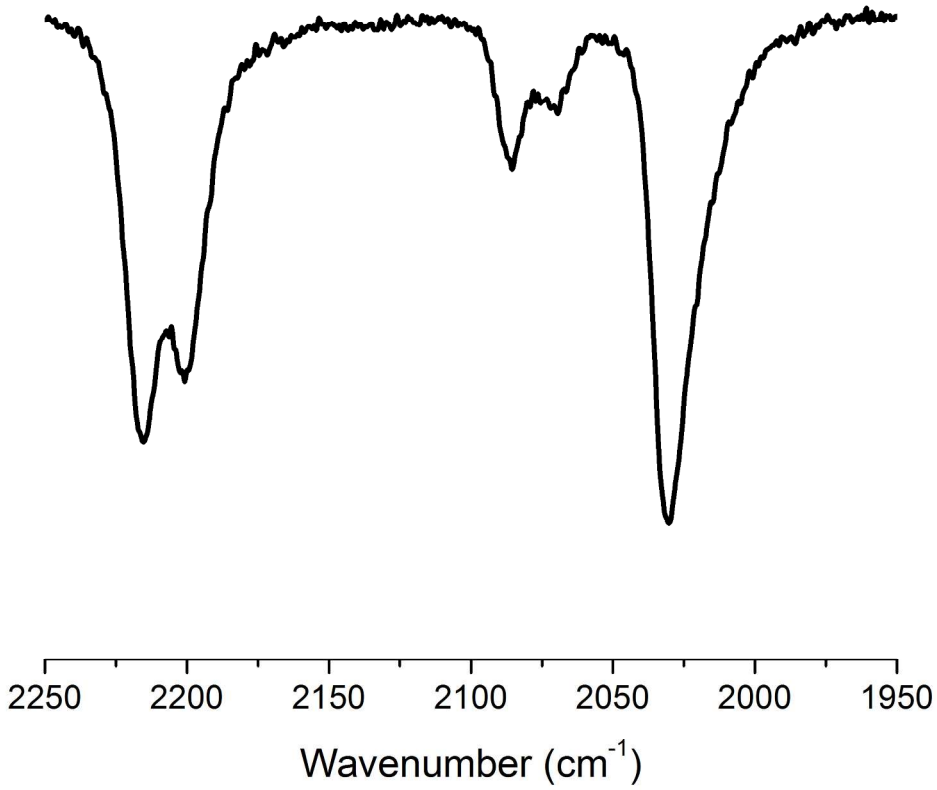

Figure S4. IR spectrum of **1**$(BAr^F{}_3)_2$ in CH_2Cl_2 solution (trans-CO/cis-CN isomer). An impurity of the cis-CO/cis-CN isomer indicated by the ν_{CO} band at 2070 cm^{-1}.

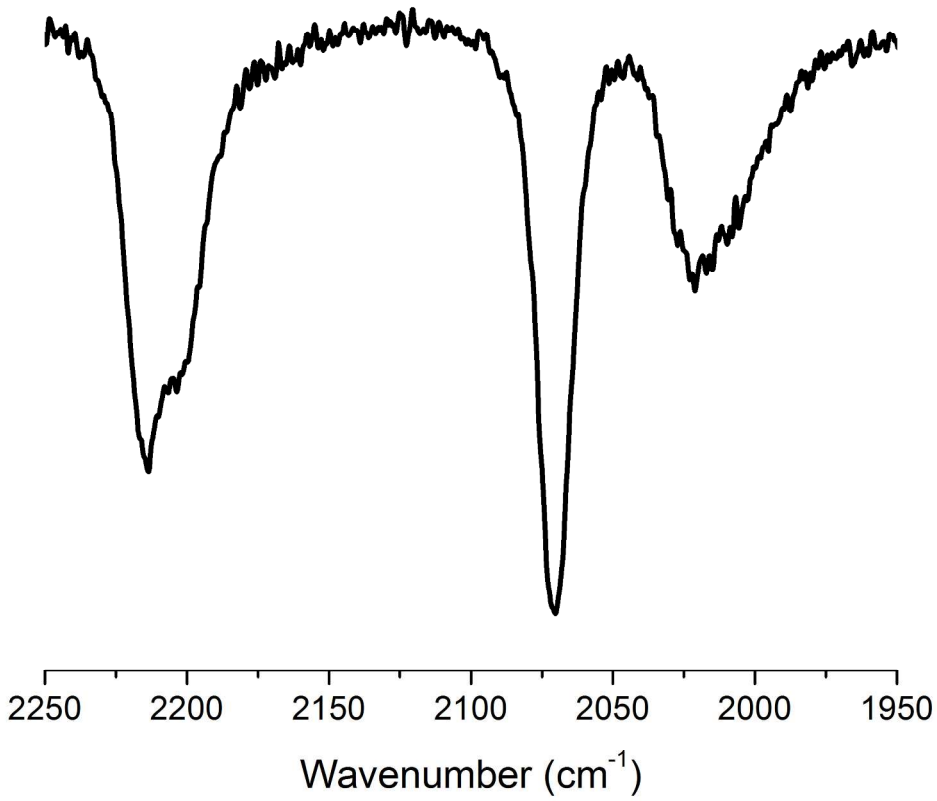

Figure S5. IR spectrum of **1**$(BAr^F{}_3)_2$ in CH_2Cl_2 solution (cis-CO/cis-CN isomer).

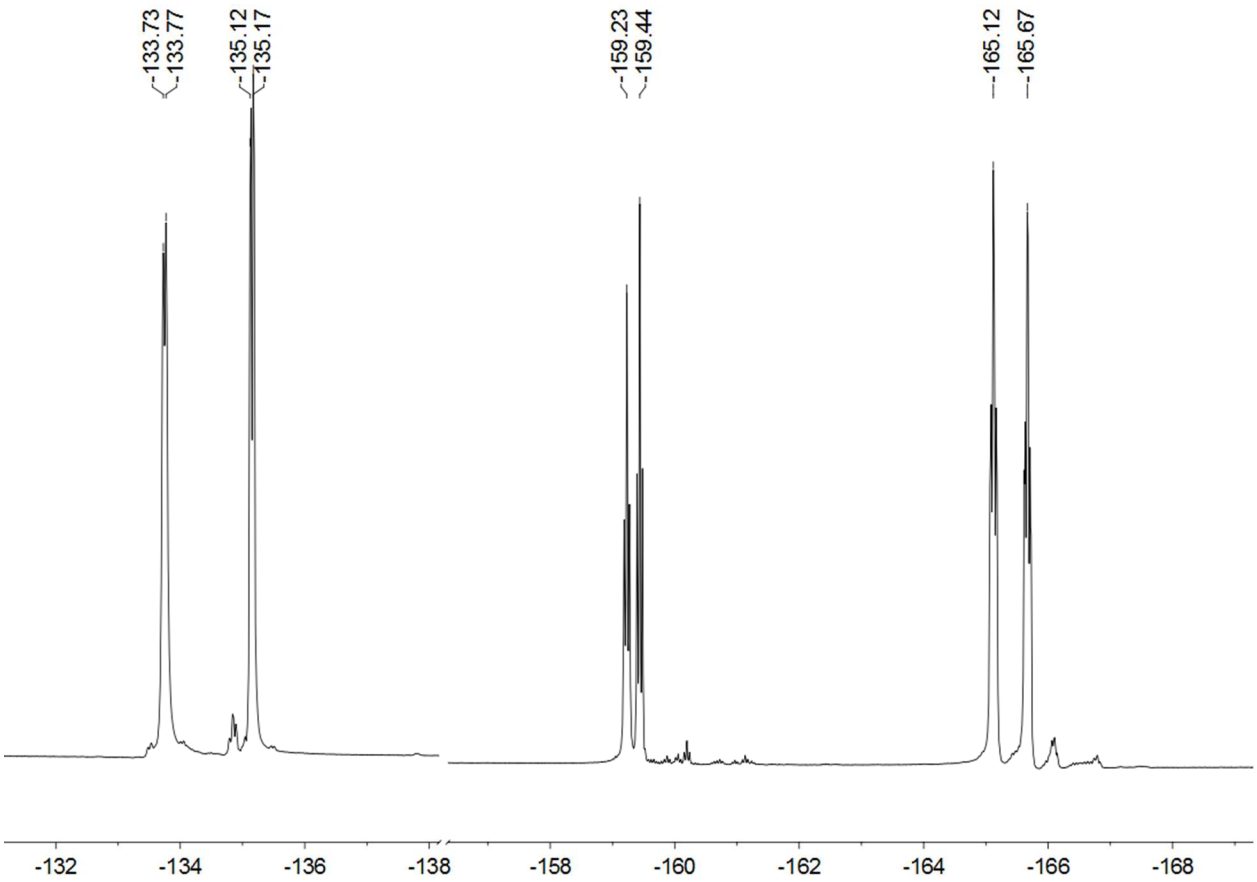

Figure S6. ^{19}F NMR spectrum of the cis-CO/trans-CN isomer of **1**$(BAr^{F}_{3})_2$ in a CD_2Cl_2 solution.

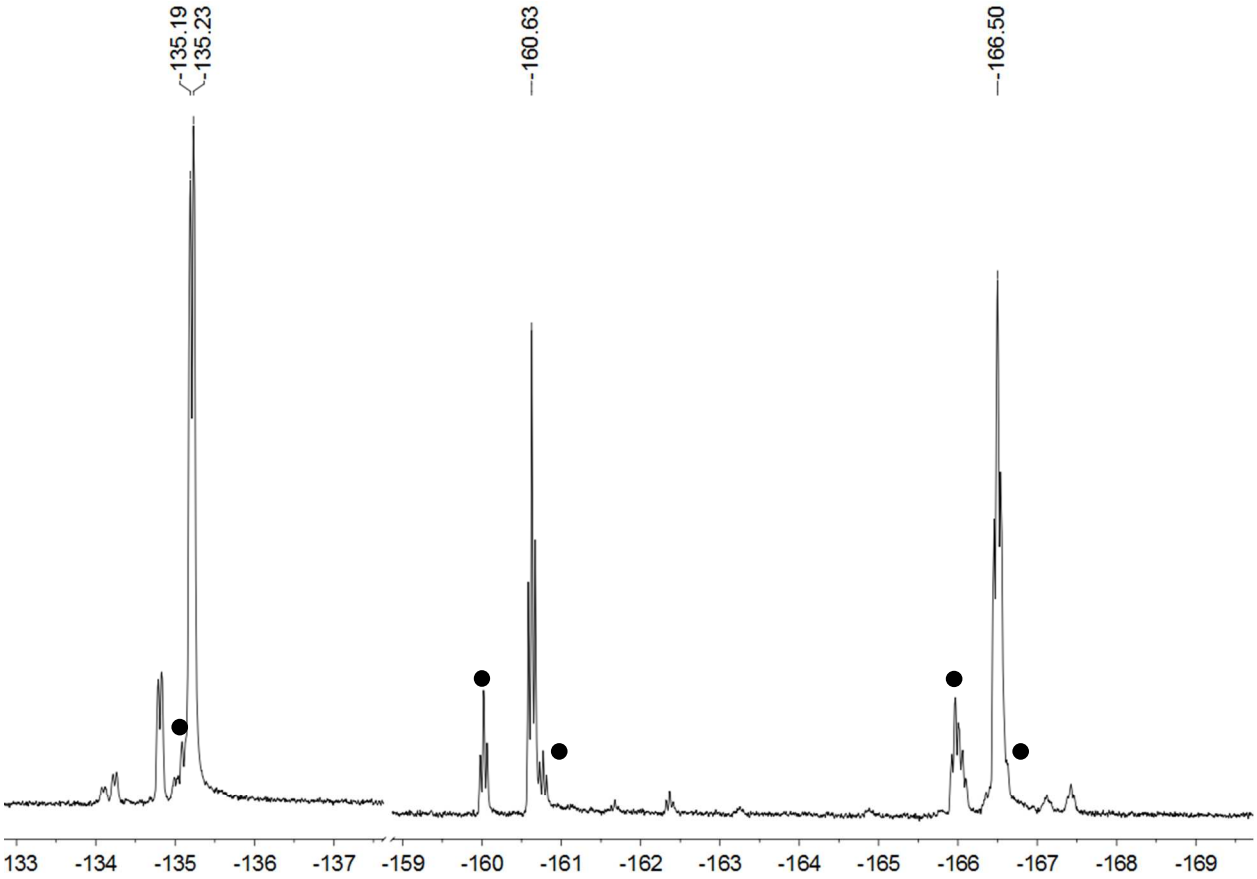

Figure S7. ^{19}F NMR spectrum of **1**$(BAr^F{}_3)_2$ showing the presence of the cis-CO/trans-CN isomer. Signals for cis-CO/cis-CN isomer of **1**$(BAr^F{}_3)_2$ also observed (●).

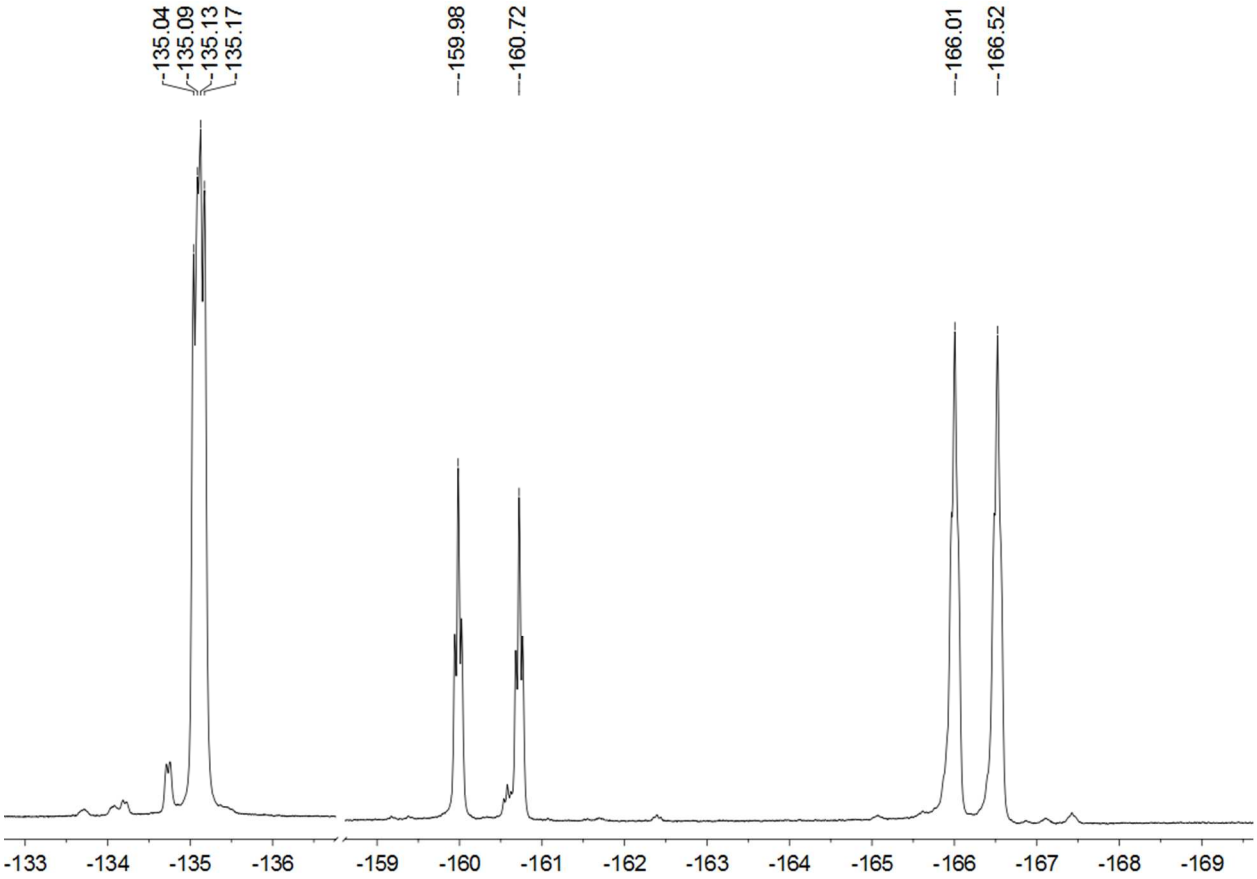

Figure S8. ^{19}F NMR spectrum of **1**$(BAr^F_3)_2$ showing the presence of the cis-CO/trans-CN isomer.

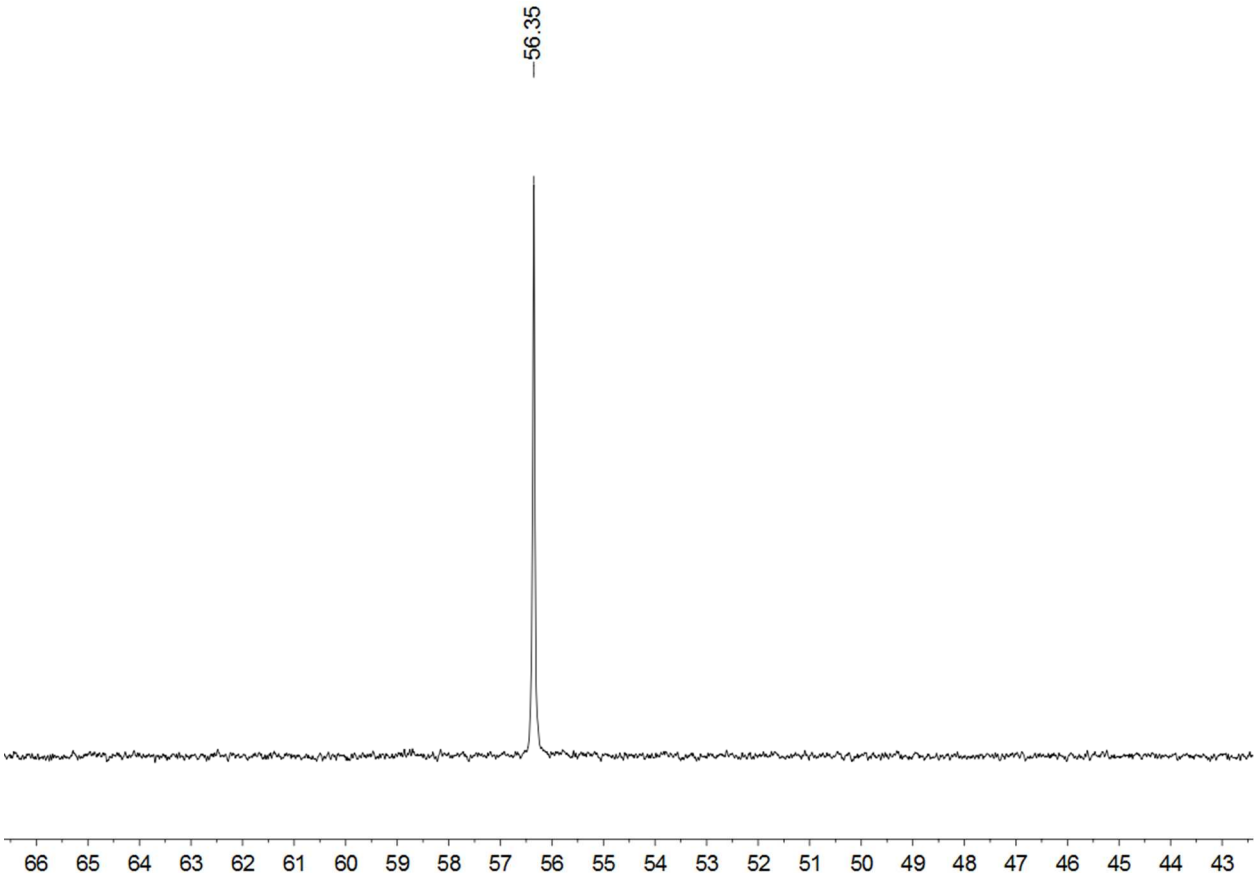

Figure S9. ^{31}P NMR spectrum of cis-CO/trans-CN isomer of **1**$(BAr^F_3)_2$ in CD_2Cl_2 solution.

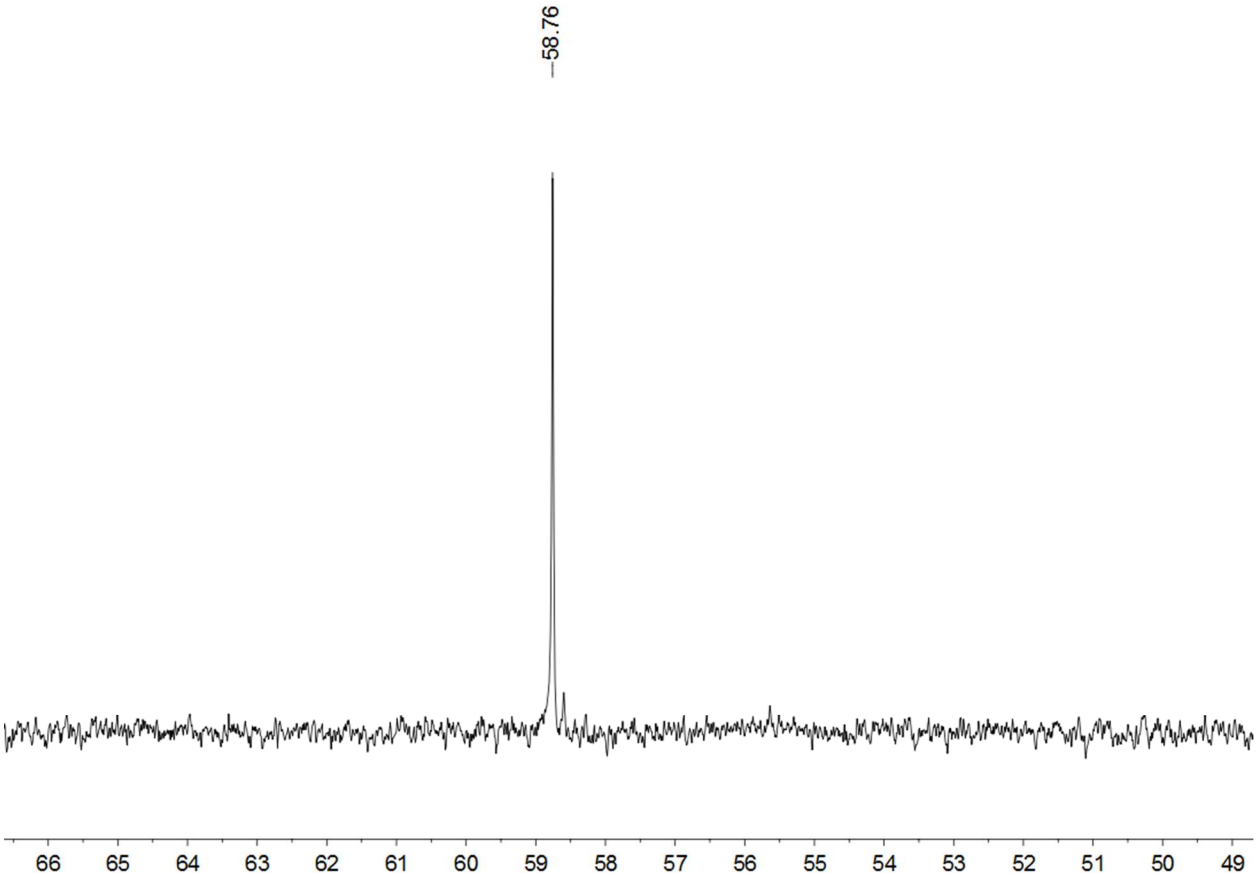

Figure S10. ^{31}P NMR spectrum of trans-CO/cis-CN isomer of **1**$(BAr^F{}_3)_2$ in CD_2Cl_2 solution.

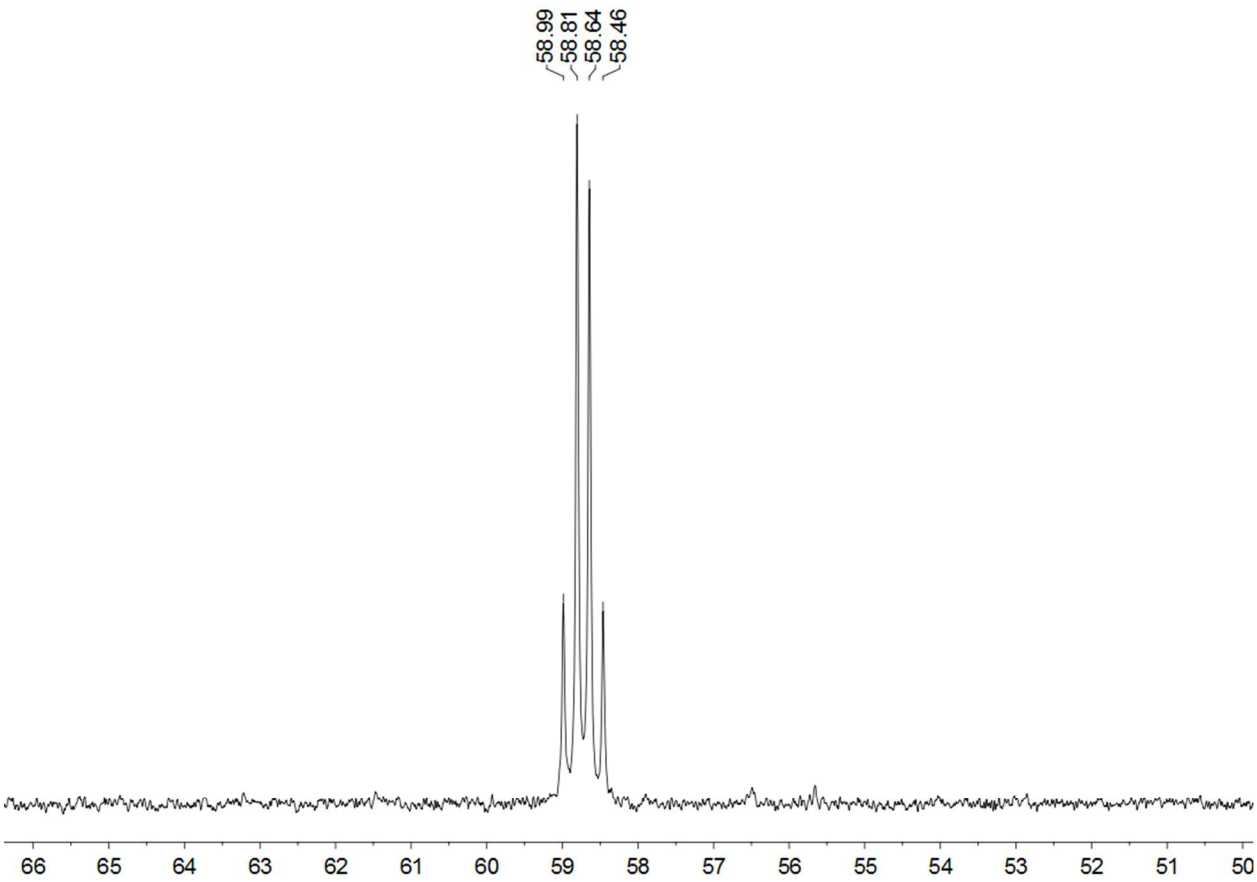

Figure S11. ^{31}P NMR spectrum of cis-CO/cis-CN isomer of **1**$(BAr^F{}_3)_2$ in CD_2Cl_2 solution.

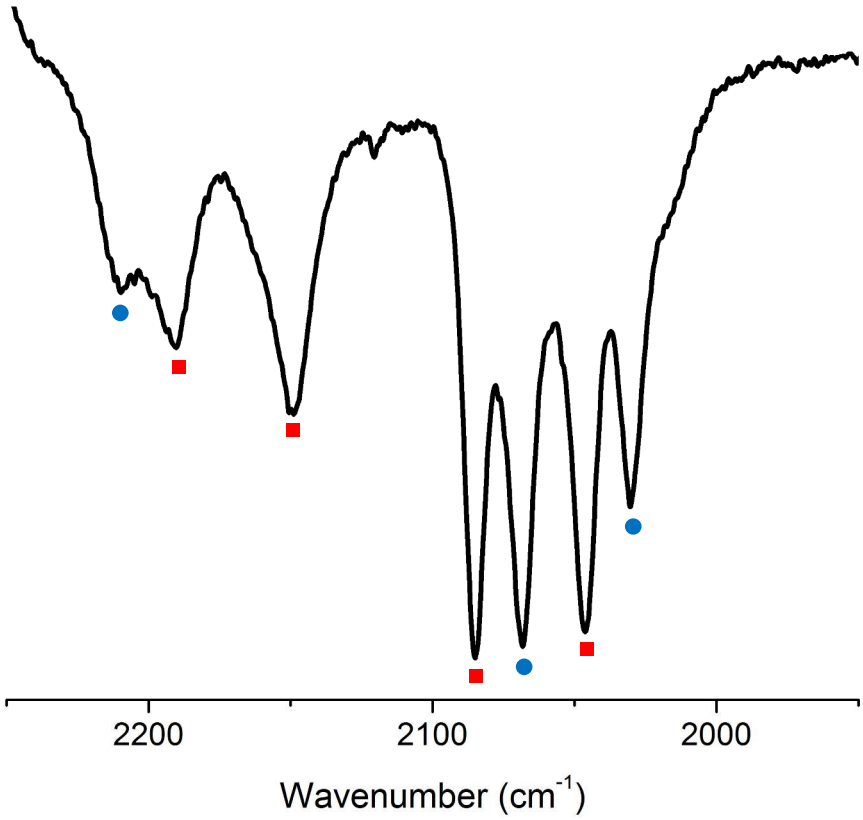

Figure S12. IR spectrum of cis-CO/trans-CN(■) and cis-CO/trans-CN(●) isomers of **2**$(BArF_3)_2$ in CH_2Cl_2 solution. A second ν_{CN} band expected for the cis-CO/cis-CN isomer is not observed.

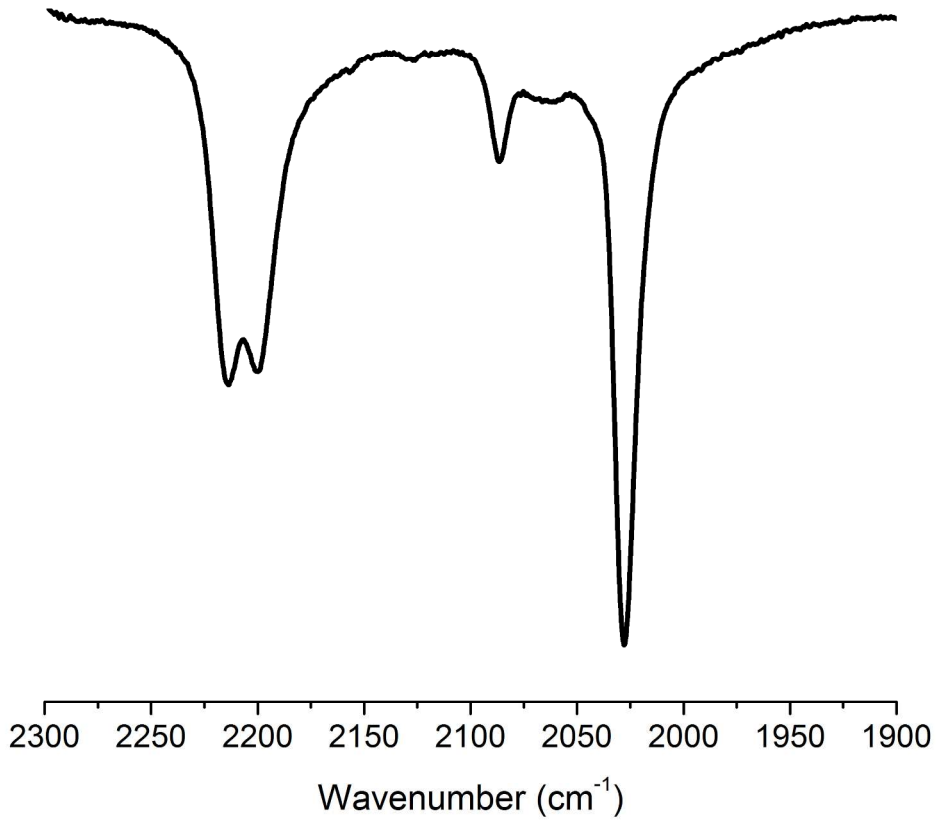

Figure S13. IR spectrum of trans-CO/cis-CN isomer of **2**$(BAr^F_3)_2$ in CH_2Cl_2 solution.

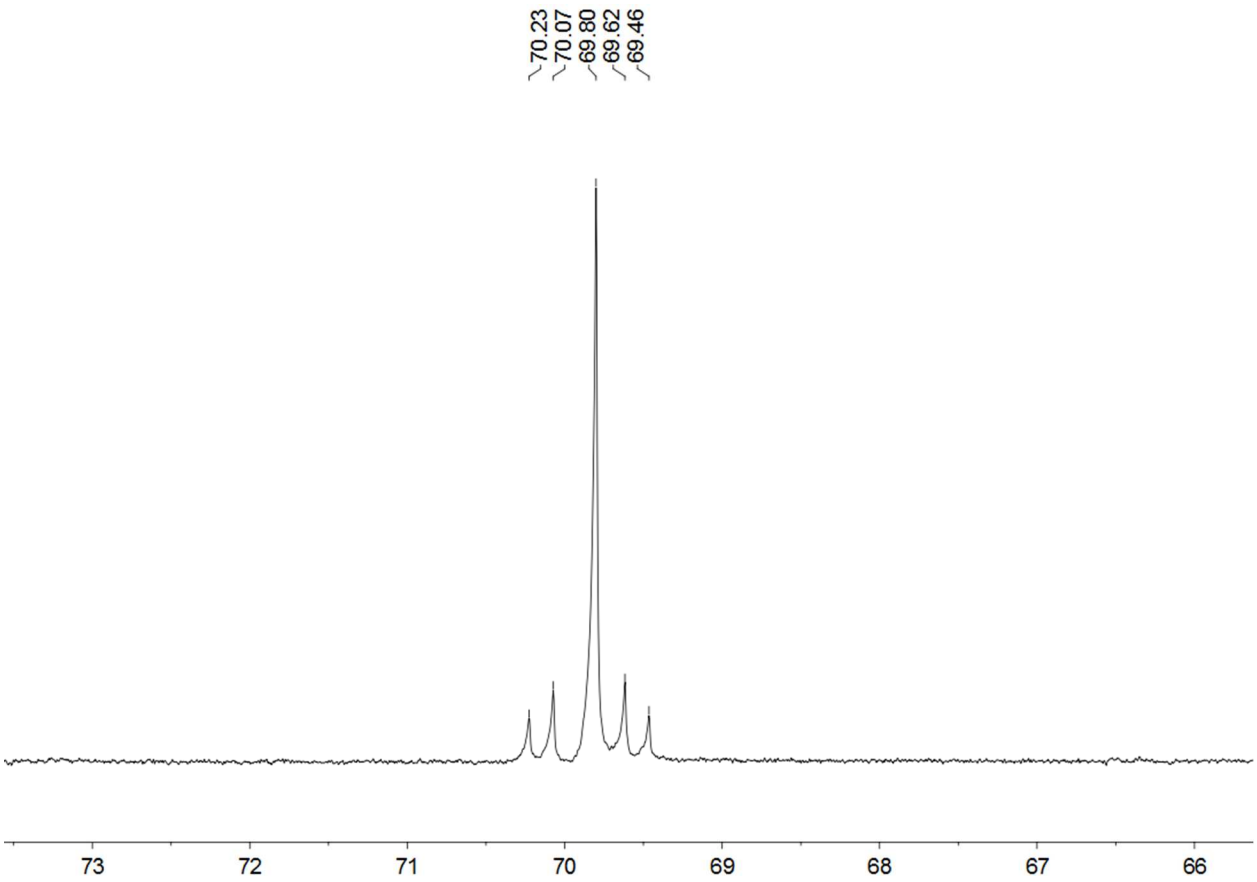

Figure S14. ^{31}P NMR spectrum of trans-CO/cis-CN and cis-CO/cis-CN isomers of **2**$(BAr^F{}_3)_2$ in CD_2Cl_2 solution.

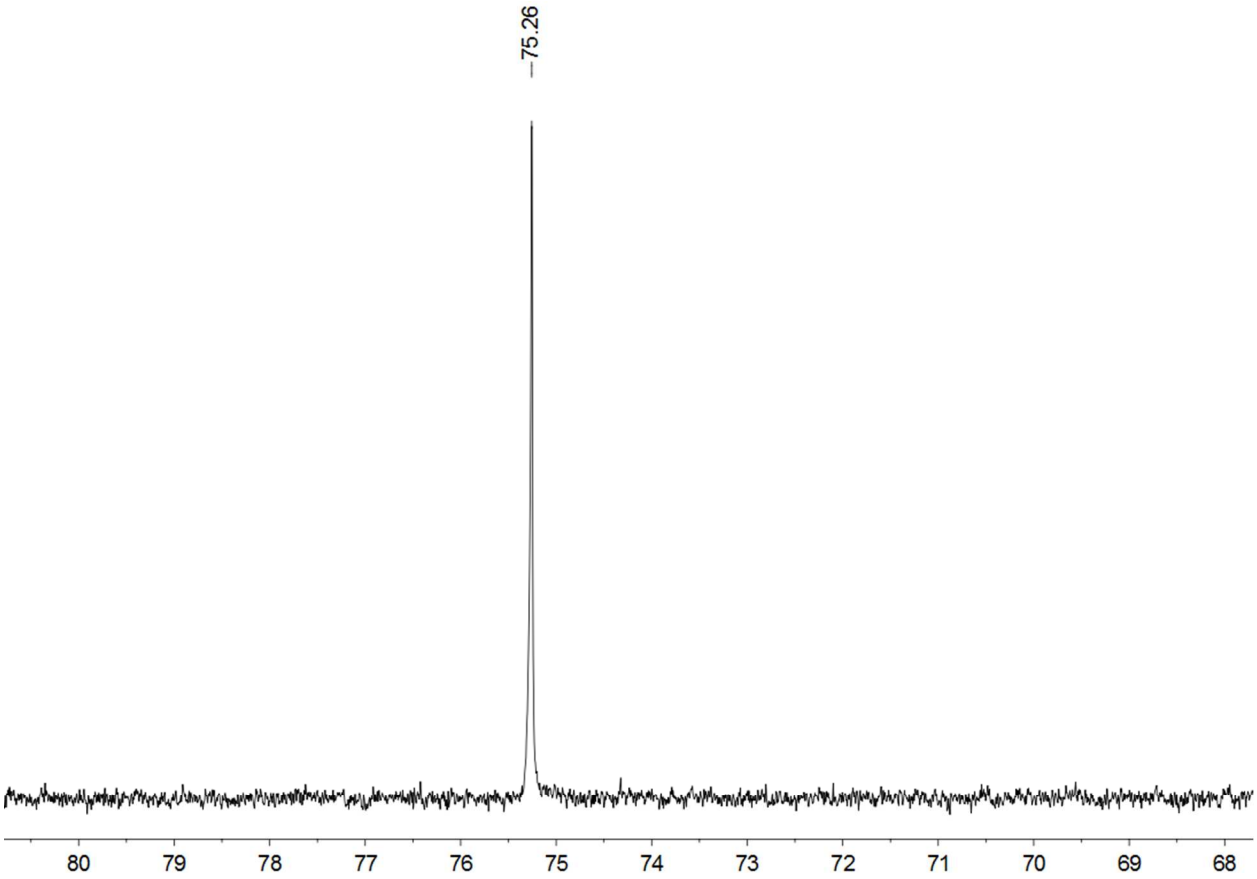

Figure S15. ^{31}P NMR spectrum of cis-CO/trans-CN isomer of **2**$(BAr^F{}_3)_2$ in CD_2Cl_2 solution.

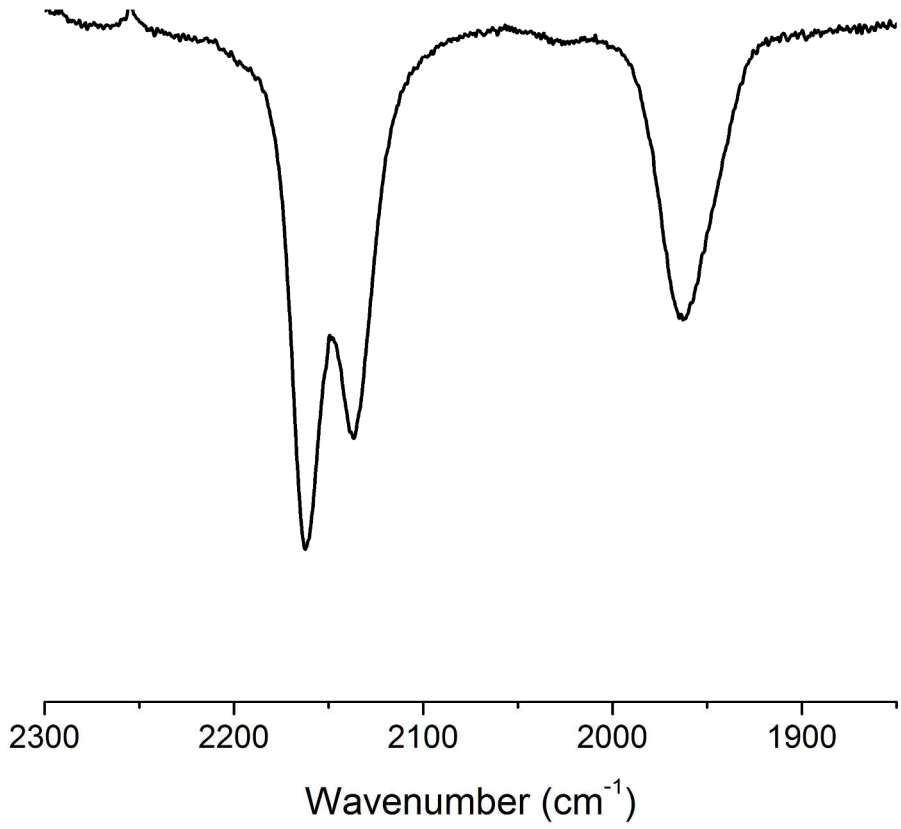

Figure S16. IR spectrum of $Et_4N[H\mathbf{3}(BAr^F{}_3)_2]$ in CH_2Cl_2 solution.

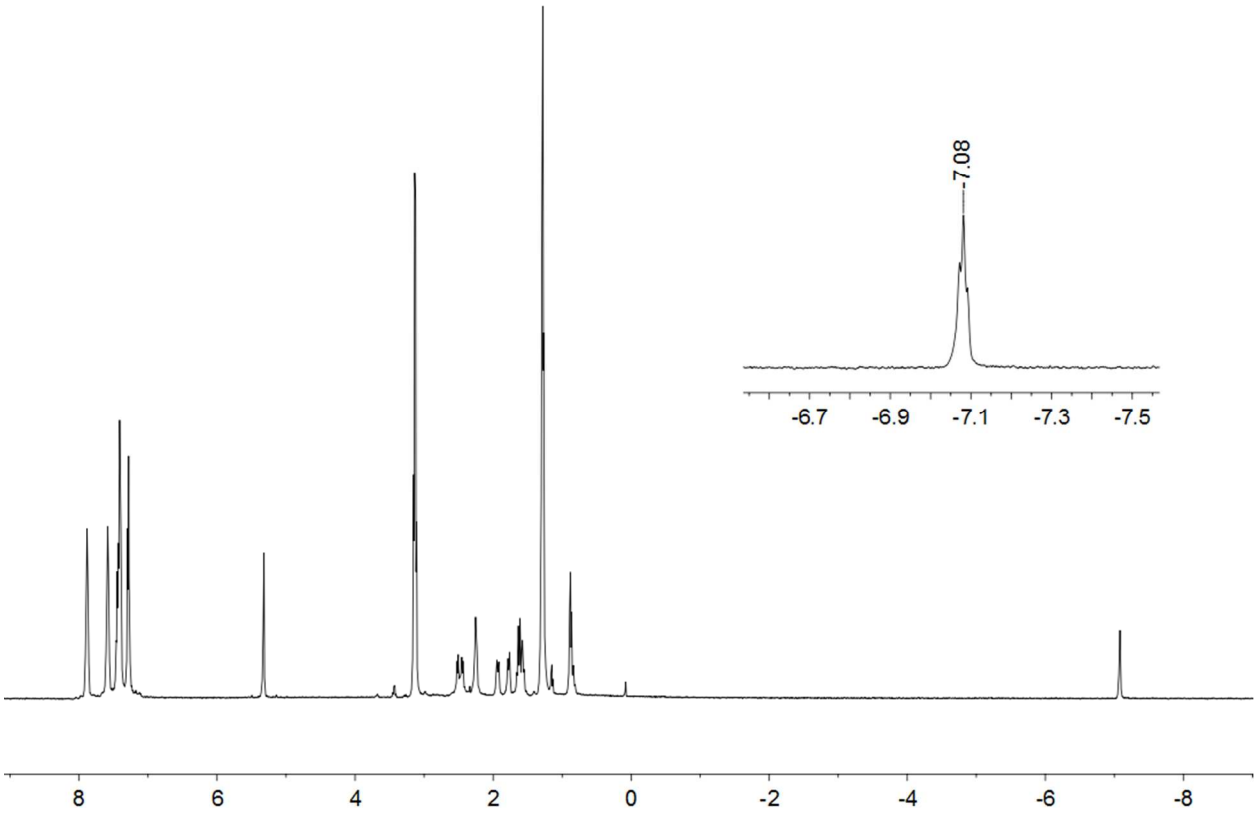

Figure S17. ^{1}H NMR spectrum of $Et_4N[H\mathbf{3}(BAr^F{}_3)_2]$ in CD_2Cl_2 solution.

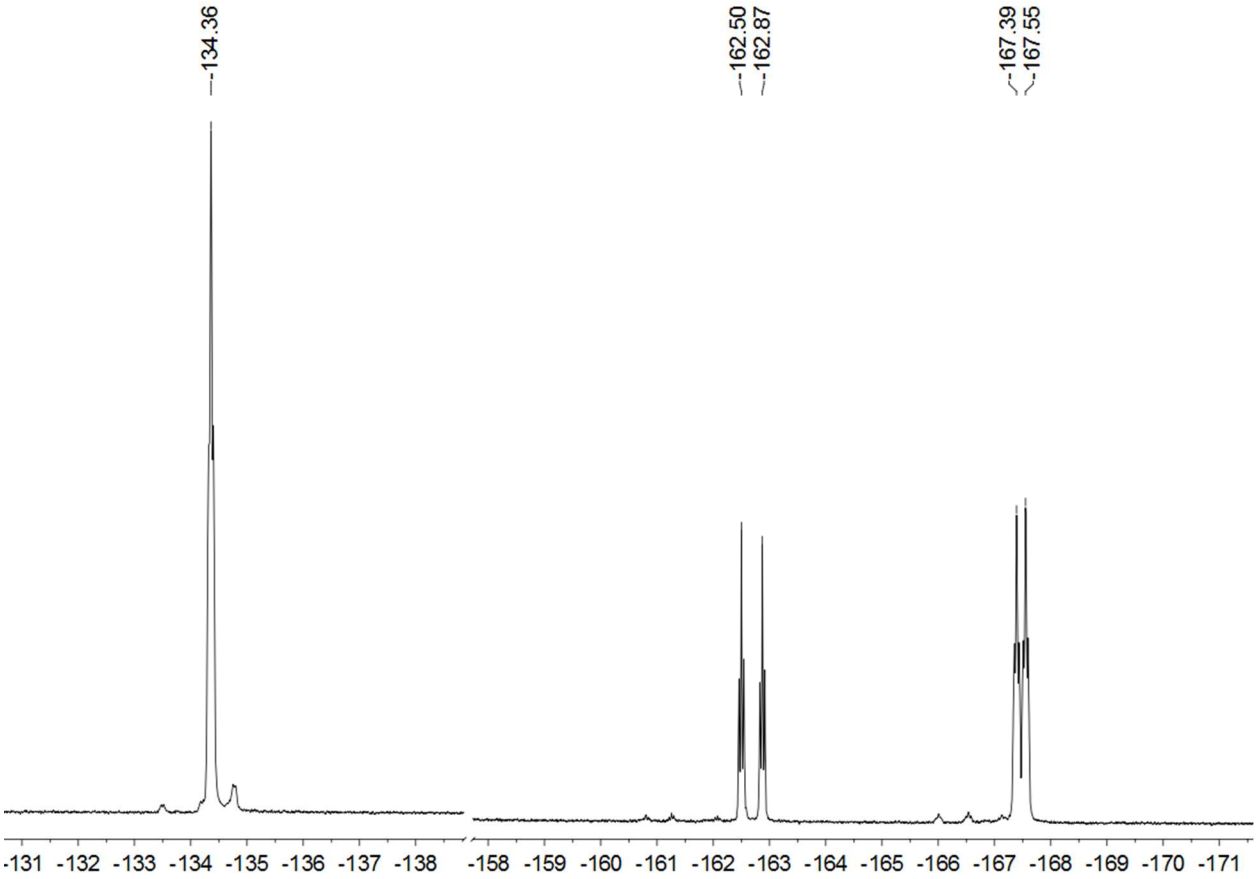

Figure S18. ^{19}F NMR spectrum of $Et_4N[H\mathbf{3}(BAr^F{}_3)_2]$ in CD_2Cl_2 solution.

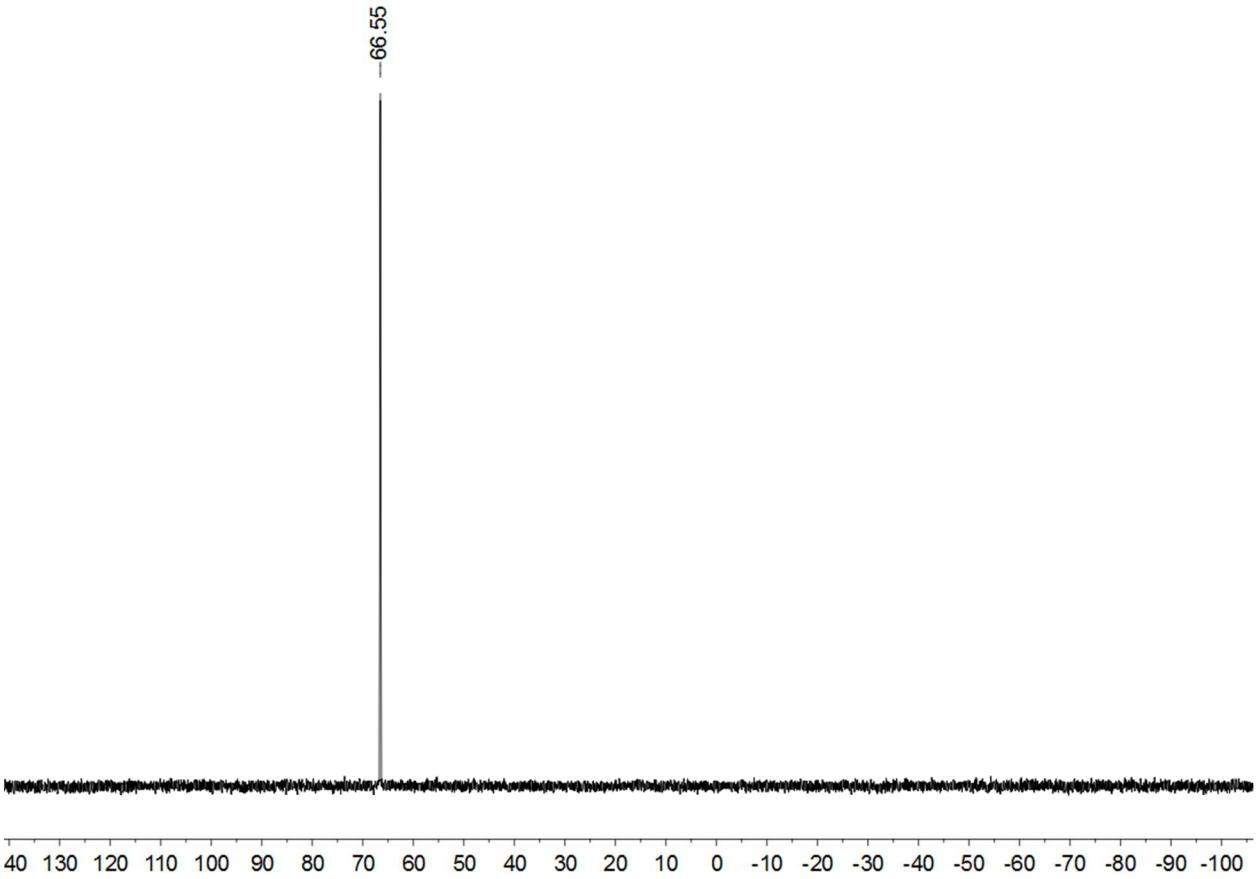

Figure S19. ^{31}P NMR spectrum of $Et_4N[H\mathbf{3}(BAr^F{}_3)_2]$ in CD_2Cl_2 solution.

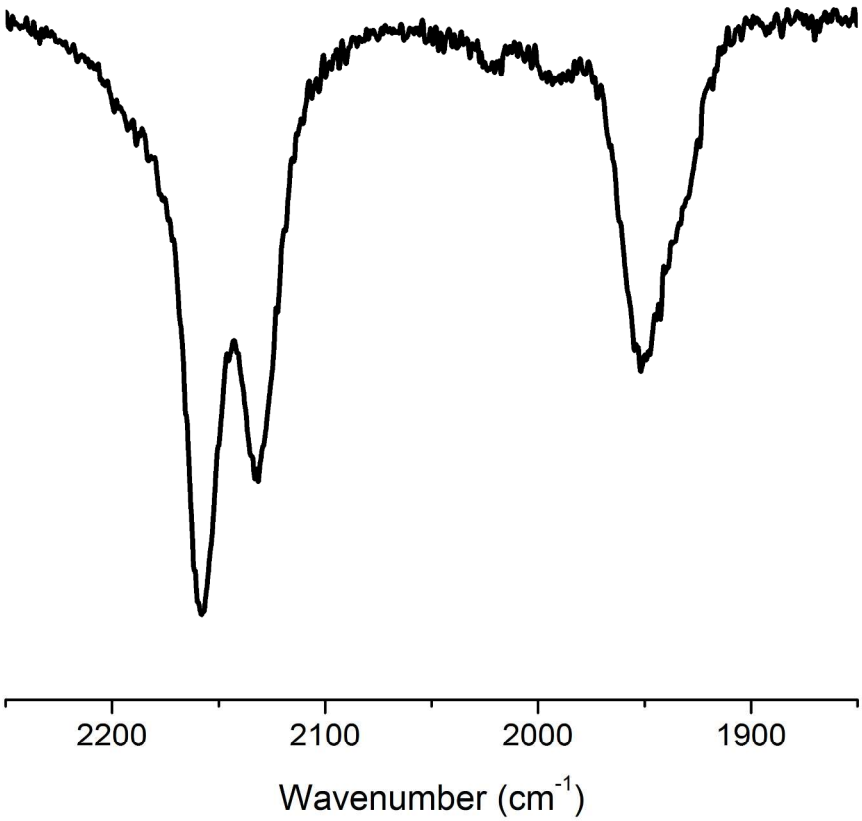

Figure S20. IR spectrum of $Et_4N[H\mathbf{4}(BAr^F{}_3)_2]$ in CH_2Cl_2 solution.

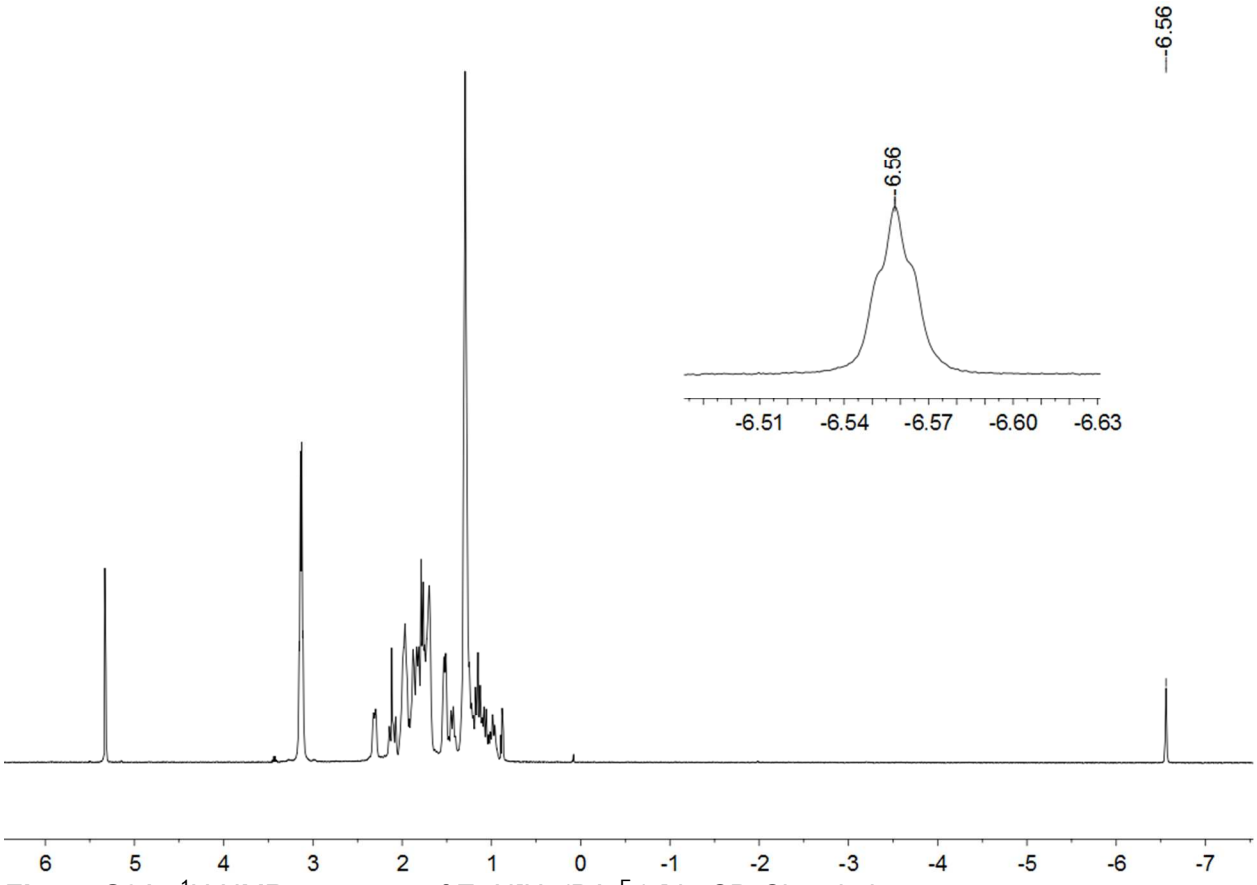

Figure S21. ^{1}H NMR spectrum of $Et_4N[H\mathbf{4}(BAr^F{}_3)_2]$ in CD_2Cl_2 solution.

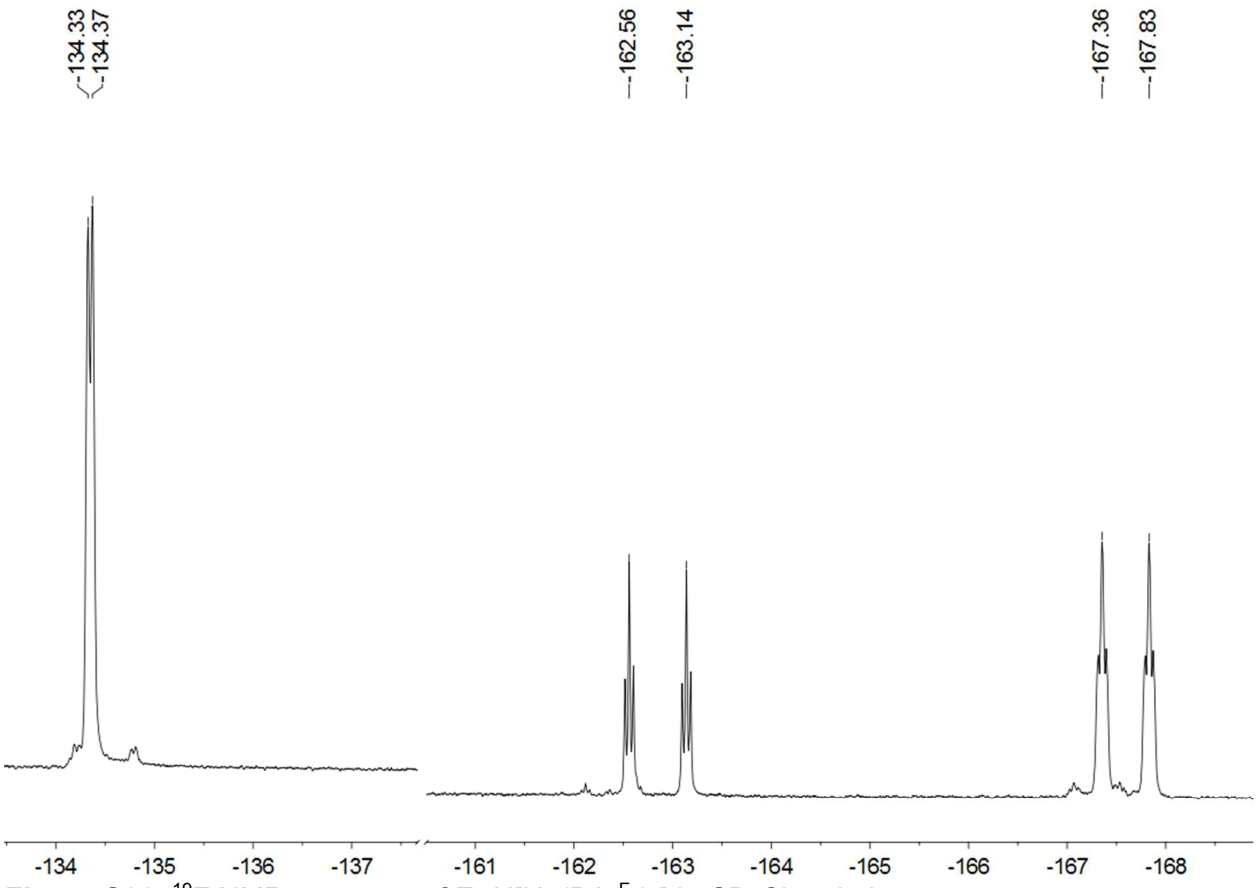

Figure S22. ^{19}F NMR spectrum of $Et_4N[H\mathbf{4}(BAr^F{}_3)_2]$ in CD_2Cl_2 solution.

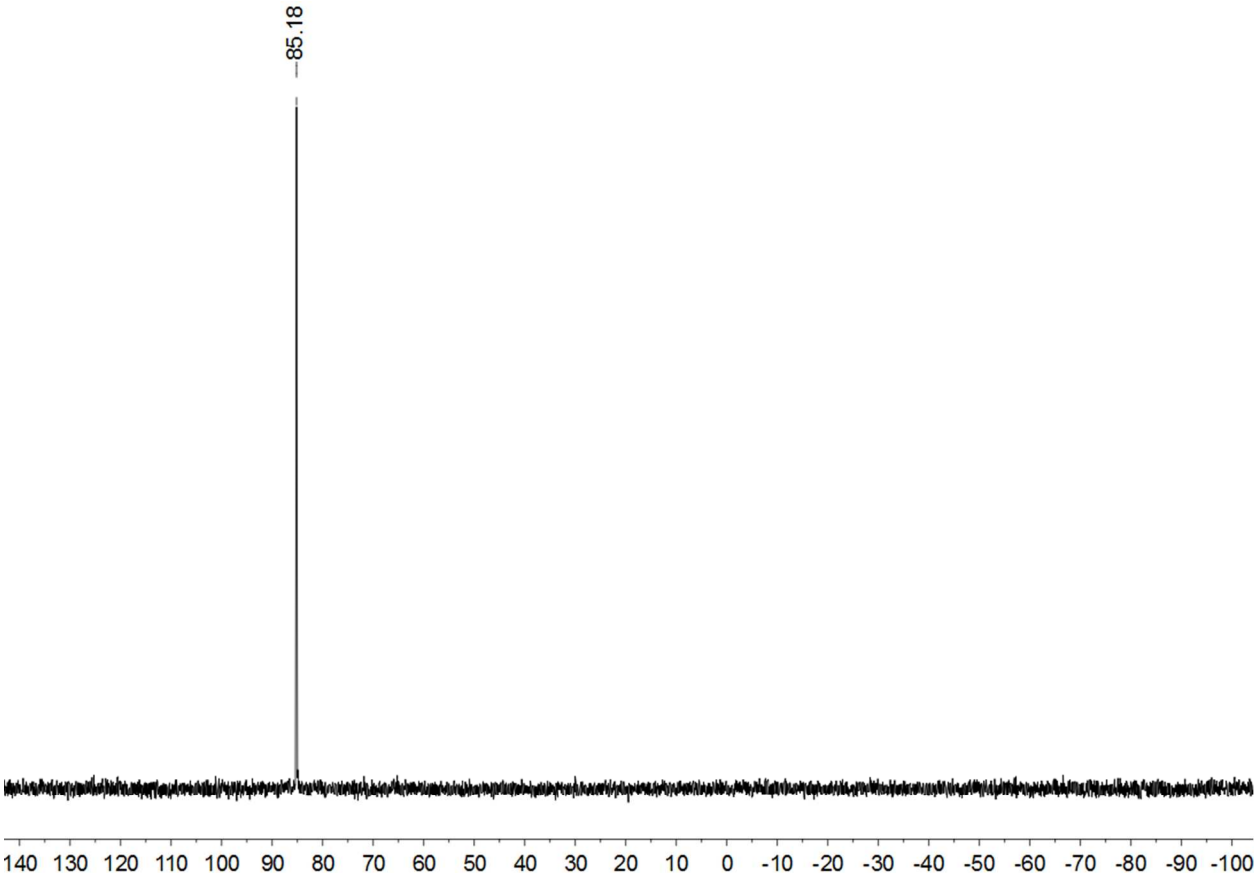

Figure S23. ^{31}P NMR spectrum of $Et_4N[H\mathbf{4}(BAr^F{}_3)_2]$ in CD_2Cl_2 solution.

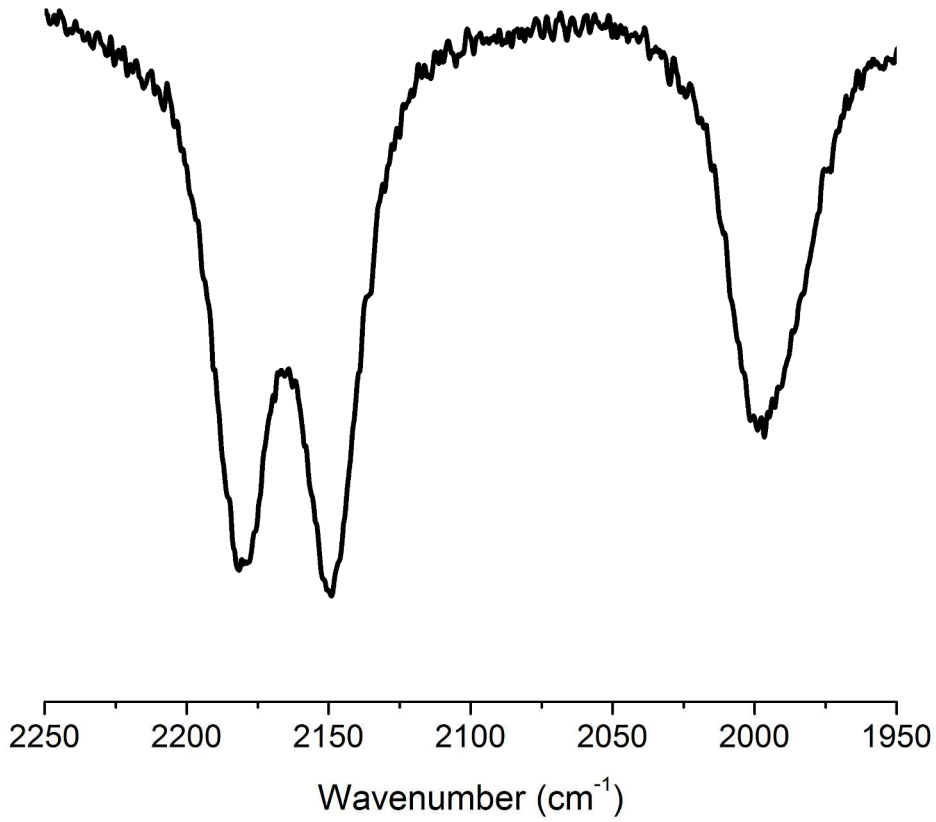

Figure S24. IR spectrum of $Et_4N[Cl\mathbf{3}(BAr^F{}_3)_2]$ in CH_2Cl_2 solution.

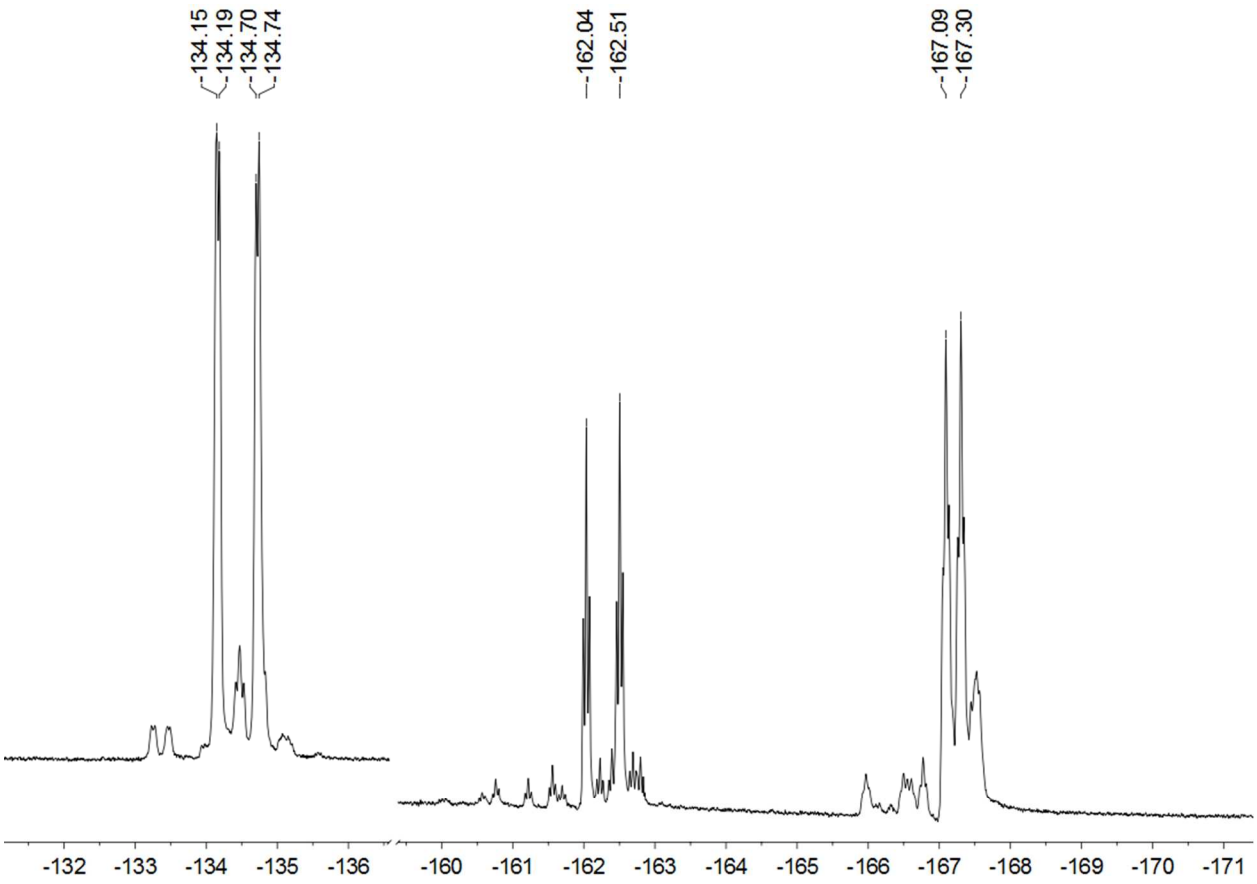

Figure S25. ^{19}F NMR spectrum of $Et_4N[Cl\mathbf{3}(BAr^F{}_3)_2]$ in CD_2Cl_2 solution.

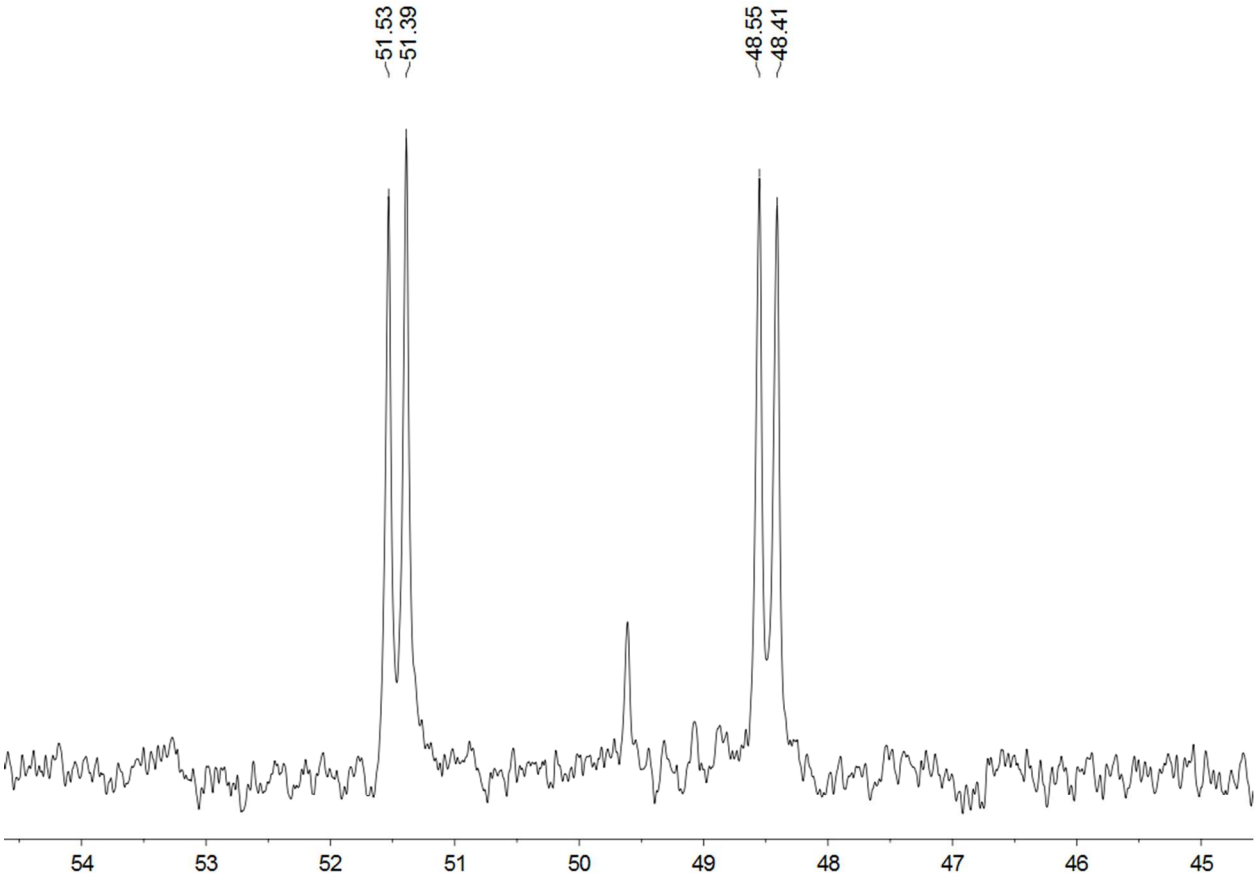

Figure S26. ^{31}P NMR spectrum of $Et_4N[Cl\mathbf{3}(BAr^F{}_3)_2]$ in CD_2Cl_2 solution.

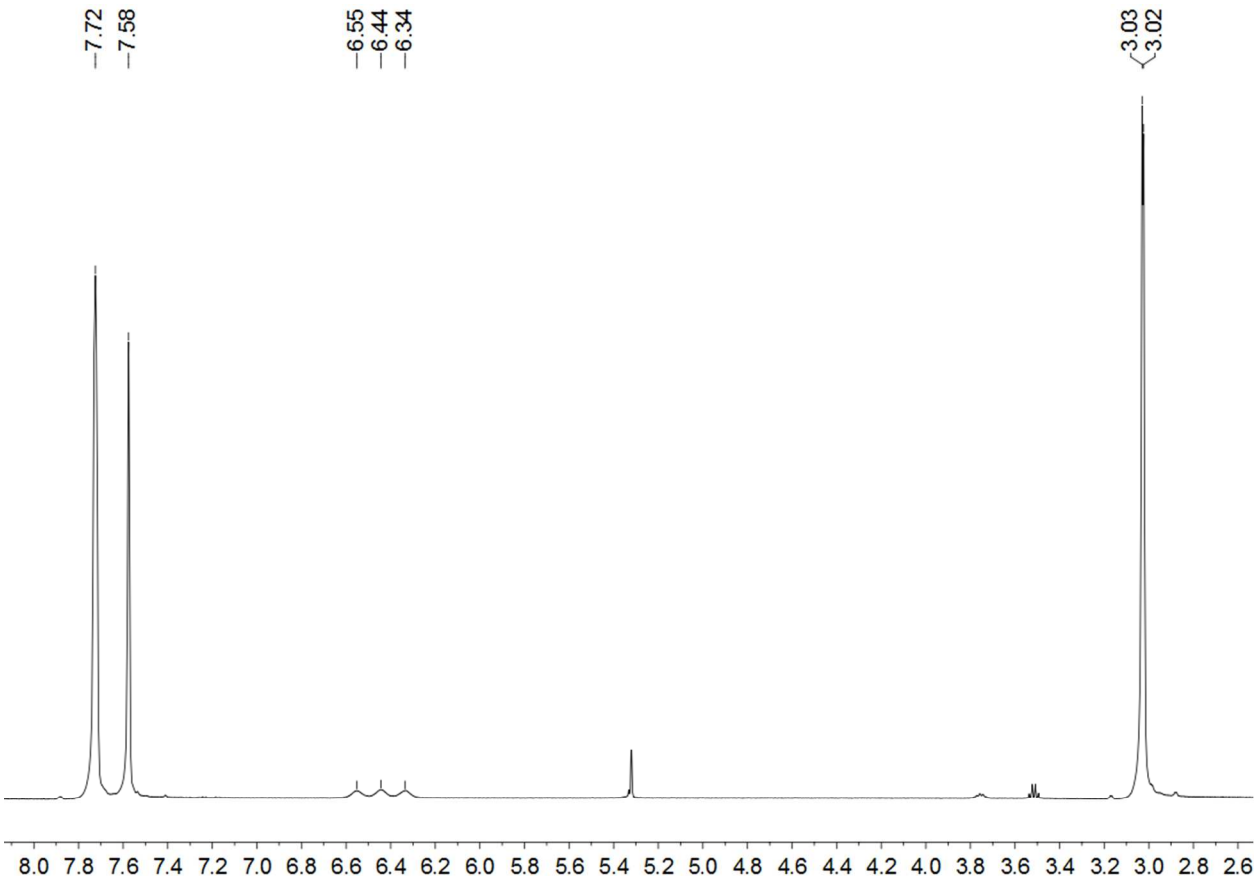

Figure S27. ^{1}H NMR spectrum of $HNMe_3BAr^{F24}$ in CD_2Cl_2 solution.

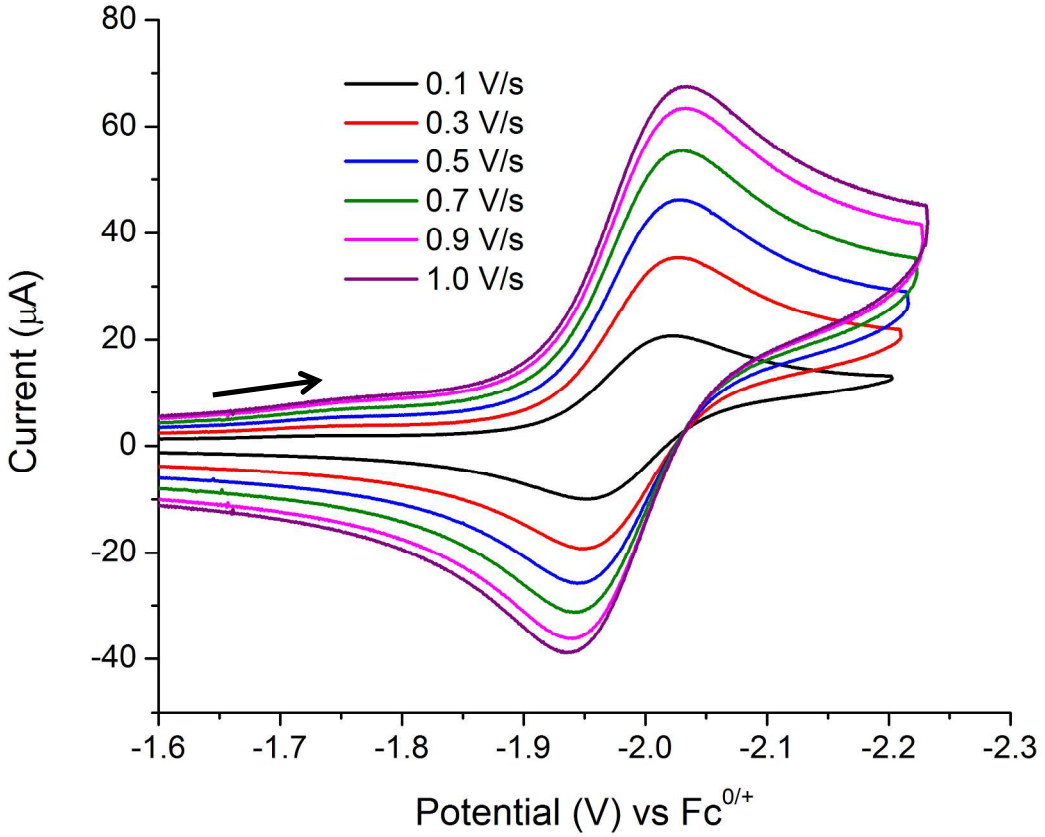

Fig S28. Cyclic voltammogram of the reduction of $Et_4N[H\mathbf{3}(BAr^F{}_3)_2]$ at varying scan rates in CH_2Cl_2 (25°C).

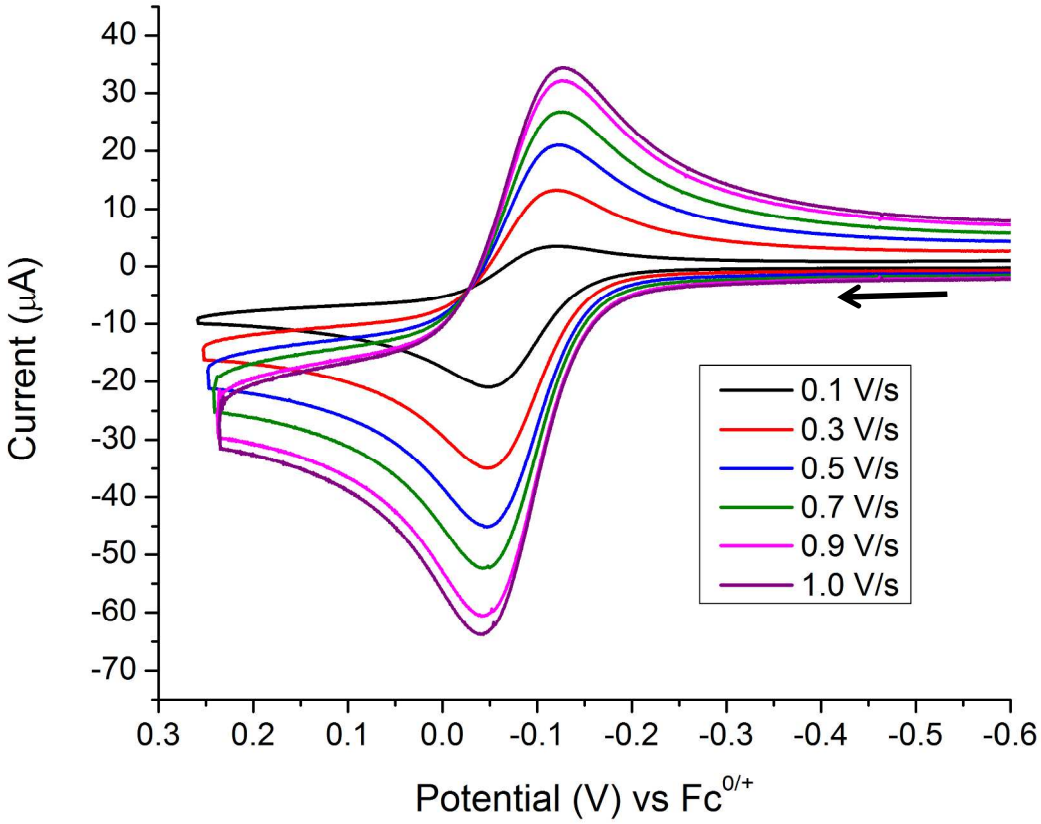

Fig S29. Cyclic voltammogram of the oxidation of $Et_4N[H\mathbf{3}(BAr^F{}_3)_2]$ at varying scan rates in CH_2Cl_2 (25°C).

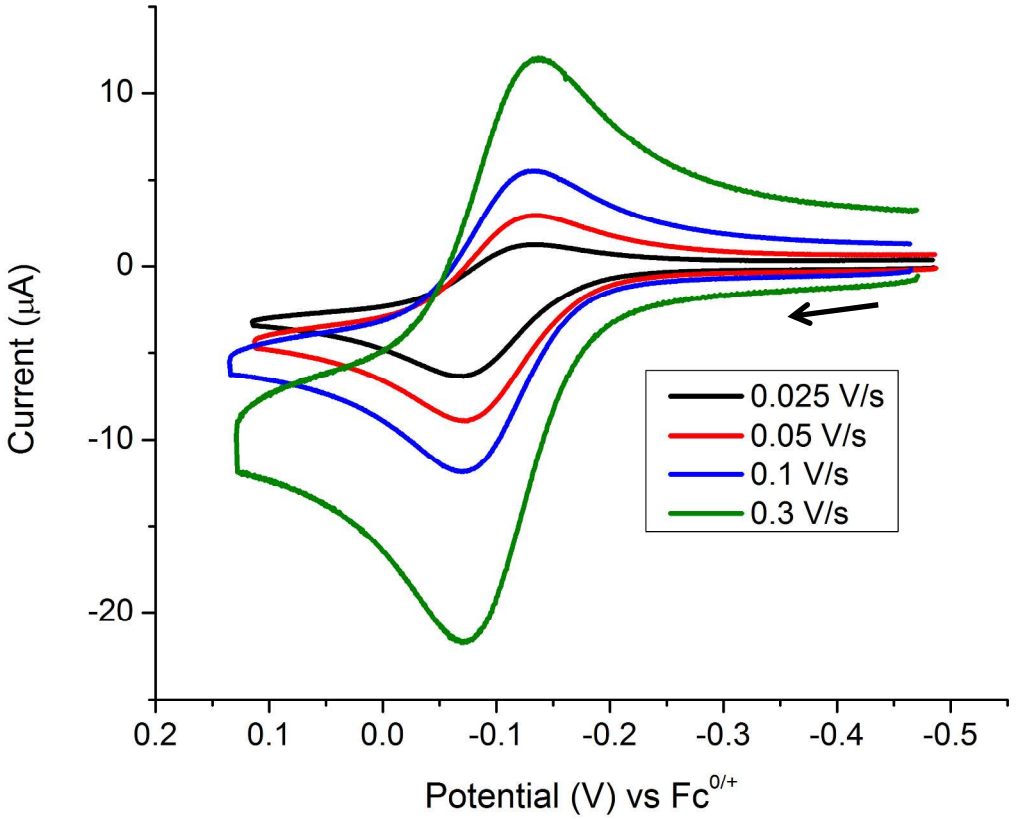

Fig S30. Cyclic voltammogram of the oxidation of $Et_4N[H\mathbf{4}(BAr^F{}_3)_2]$ at varying scan rates in CH_2Cl_2 (25°C).

Determination of the equilibrium constant for dihydrogen bonding:

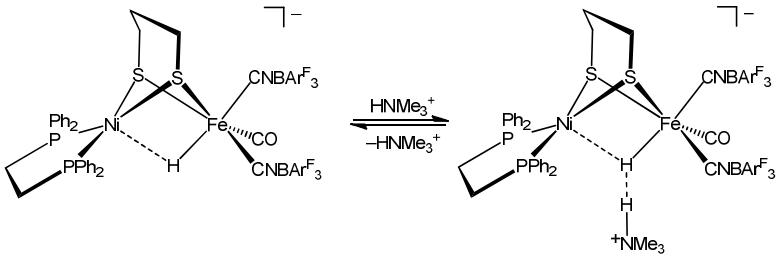

A plot of δ_{obs} vs $[HNMe_3^+]_o$ was fit by the equation:[5]

$$\delta_{obs} = \delta_{MH} + \frac{1}{2[MH]_o}(\delta_{MHHN} - \delta_{MH})\left[\left([MH]_o + [HN]_o + {}^1/_K\right) - \sqrt{\left([MH]_o + [HN]_o + {}^1/_K\right)^2 - 4[MH]_o[HN]_o}\right]$$

Where:

δ_{obs} = Observed hydride chemical shift of in the presence of $HNMe_3^+$

δ_{MH} = Hydride chemical shift of [H**3**$(BAr^F{}_3)_2$] in the absence of $HNMe_3^+$

δ_{MHHN} = Hydride chemical shift of [H**3**$(BAr^F{}_3)_2$] in the presence of excess $HNMe_3^+$

$[MH]_o$: Initial concentration of [H**3**$(BAr^F{}_3)_2$]

$[HN]_o$: Initial concentration of $HNMe_3^+$

K = Equilibrium constant for formation of a dihydrogen bond between [H**3**$(BAr^F{}_3)_2$] and $HNMe_3^+$

Table S2. ^{1}H NMR signals for the titration of Et_4N[H**3**$(BAr^F{}_3)_2$] with $HNMe_3BAr^{F24}$

mol $HNMe_3^+$	$[HNMe_3^+]$ (M)	δ (ppm)
0	0	-7.09
1.4E-6	1.4E-3	-8.69
2.8E-6	2.8E-3	-9.03
4.2E-6	4.2E-3	-9.11
5.6E-6	5.6E-3	-9.16

The unknown values of δ_{MHHN} and K were determined by a nonlinear fit of experimental values using the Leven-Marquardt algorithm. The values were determined to be δ_{MHHN} = −9.20±0.02 ppm and K = 9.0±1.0 x 10^4 L/mol.

Table S3. H_2 Production from Et_4N[H**3**$(BAr^F{}_3)_2$] and $PhNH_3BAr^{F24}\cdot 2Et_2O$

Run	Mass of Et_4N[H**3**$(BAr^F{}_3)_2$] (mg)	μmol Et_4N[H**3**$(BAr^F{}_3)_2$]	μmol of H_2 detected	mol% H_2
1	3.0	1.62	1.69	104%
2	3.0	1.62	1.51	93%
3	3.3	1.78	1.91	107%

Calculated mol% of H_2 = 101±7%

Electrocatalytic Oxidation of H_2

To a 1mM solution of $Et_4N[H\mathbf{3}(BAr^F{}_3)_2]$ in CH_2Cl_2 with 100 mM Bu_4NPF_6, aliquots of a standard DBU solution in CH_2Cl_2 (0.26 M, 0.193 mL of DBU in 5 mL of CH_2Cl_2) were added. H_2 gas was bubbled through the solution for 5 min immediately prior to scans.

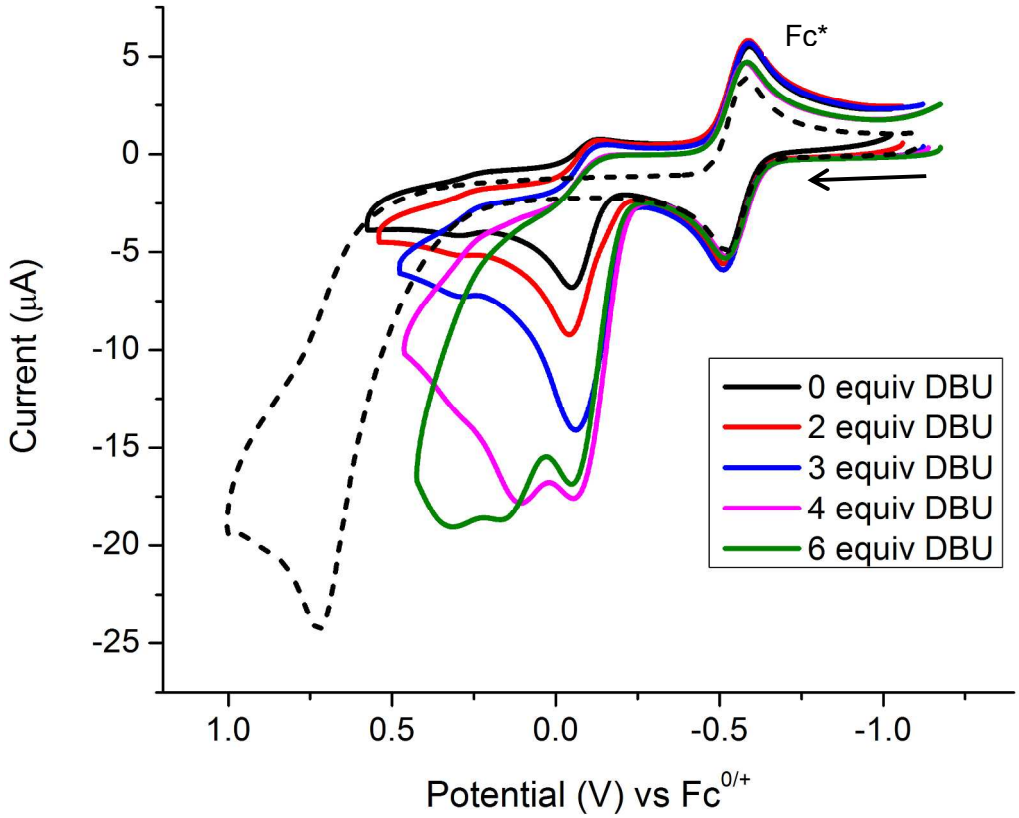

Fig S31. Cyclic voltammogram of the oxidation of $Et_4N[H\mathbf{3}(BAr^F{}_3)_2]$ in CH_2Cl_2 with increasing amounts of DBU under 1 atm of H_2 at a scan rate at 0.05 V/s (25°C). Decamethylferrocene (Fc*) used as an internal reference (□0.55 V vs $Fc^{0/+}$). 6 equiv of DBU with 1 atm of H_2 in the absence of $Et_4N[H\mathbf{3}(BAr^F{}_3)_2]$ shown in dashed black line.

Turnover frequency (k_{obs}) of 0.98 s^{-1} was determined by the method described by Bullock *et al.* (*Nat. Chem.* **2013**, *5*, 228-233).

$$\frac{i_{cat}}{i_p} = \frac{n}{0.4463}\sqrt{\frac{RTk_{obs}}{Fv}}$$

i_{cat} = maximum peak height in the presence of base
i_p = peak height in the absence of base
R = gas constant
T = temperature in Kelvin
F = Faraday's constant
v = scan rate (V/s)

References

(1) Barton, B. E.; Whaley, C. M.; Rauchfuss, T. B.; Gray, D. L. *"Nickel-Iron-Dithiolato-Hydrides Relevant to the [NiFe]-Hydrogenase Active Site" J. Am. Chem. Soc.* **2009**, *131*, 6942.

(2) Carroll, M. E.; Barton, B. E.; Gray, D. L.; Mack, A. E.; Rauchfuss, T. B. *"Active-Site Models for the Nickel-ìIron Hydrogenases: Effects of Ligands on Reactivity and Catalytic Properties" Inorg. Chem.* **2011**, *50*, 9554.

(3) Kayal, A.; Rauchfuss, T. B. *"Protonation studies of the new iron carbonyl cyanide trans-Fe(CO)(3)(CN)(2) (2-): Implications with respect to hydrogenases" Inorganic Chemistry* **2003**, *42*, 5046.

(4) Li, Z.; Ohki, Y.; Tatsumi, K. *"Dithiolato-Bridged Dinuclear Iron-Nickel Complexes [Fe(CO)2(CN)2(m-SCH2CH2CH2S)Ni(S2CNR2)]- Modeling the Active Site of [NiFe] Hydrogenase" J. Am. Chem. Soc.* **2005**, *127*, 8950.

(5) Donghi, D.; Beringhelli, T.; D'Alfonso, G.; Mondini, M. *"NMR investigation of the dihydrogen-bonding and proton-transfer equilibria between the hydrido carbonyl anion HRe2(CO)(9) (-) and fluorinated alcohols" Chemistry-a European Journal* **2006**, *12*, 1016.